A Variational Principle for the Formulation of Partitioned Structural Systems

K. C. Park and Carlos A. Felippa

Department of Aerospace Engineering Sciences
and Center for Aerospace Structures
University of Colorado, Campus Box 429
Boulder, CO 80309, USA

February 1999/ Minor Update June 2004

ABSTRACT

A continuum-based variational principle is presented for the formulation of the discrete governing equations of partitioned structural systems. This application includes coupled substructures as well as subdomains obtained by mesh decomposition. The present variational principle is derived by a series of modifications of a hybrid functional originally proposed by Atluri for finite element development. The interface is treated by a displacement frame and a localized version of the method of Lagrange multipliers. Interior displacements are decomposed into rigid-body and deformational components to handle floating subdomains. Both static and dynamic versions are considered. An important application of the present principle is the treatment of nonmatching meshes that arise from various sources such as separate discretization of substructures, independent mesh refinement, and global-local analysis. The present principle is compared with that of a globalized version of the multiplier method.

1. INTRODUCTION

The decomposition of discrete models of mechanical systems has received increased attention in recent years. Research into that topic has been driven by the analysis of coupled systems, the solution of inverse problems and the use of massively parallel computers. This paper studies a specific class of decompositions: the partitioned analysis of mechanical systems.

The term *partitioning* identifies the process of *spatial* separation of a discrete mechanical model into interacting components generically called *partitions*. The decomposition may be driven by physical, functional, or computational considerations. For example, the structure of a complete airplane can be decomposed into substructures such as wings and fuselage according to *function*. Substructures can be further decomposed into submeshes or subdomains to accommodate parallel *computing* requirements. Going the other way, if that flexible airplane is part of a flight simulation, a top-level partition driven by *physics* consists of fluid and structure (and perhaps control and propulsion) models. This kind of multilevel partition hierarchy, viz., coupled system, structure, substructure and subdomain, is typical of present practice in modeling and computational technology.

Partitioned analysis stipulates that the discretization of individual components through standard methods (such as finite elements, finite differences or boundary elements) is well on hand. The problem is thereby reduced to modeling the *interaction* of those components. For simple decompositions, as in a mechanical mesh collocated to another, this can be handled by well known primal or dual techniques, such as degree of freedom matching or standard Lagrange multipliers.

Complications may be introduced into the picture, however, by several factors. Physically heterogeneous models may be the product of different discretization techniques, as exemplified by a pressure-based fluid BEM mesh coupled to a displacement-based FEM structural mesh. Nodes on both sides of an interface may be nonmatching, sliding or moving; the latter being typical of contact and impact problems. Finally, multilevel decompositions bring combinatorial complexity.

A source of nonmatching meshes is illustrated in Figure 1. The domain Ω of Figure 1(a) is divided into three subdomains by an interface $\partial\Omega_b$ as depicted in Figure 1(b). Figure 1(c) shows a FEM discretization with matching meshes. This typically results by discretizing the whole domain first, followed by mesh decomposition. If subdomain meshes are subsequently refined without consideration of interconnections, nonmatching meshes may result as pictured in Figure 1(d). Note that if the interface segments are curved as in this example, the discrete interfaces do not generally overlap in space and their normals are generally misaligned.

To handle such a wide variety of scenarios it is useful to develop a general continuum variational framework, from which specific partitioned formulations and solution algorithms can be developed and tested. The situation is analogous to the transition that took place in the development of the finite element method from matrix structural analysis to continuum-based variational principles, which are by now well established. These "coupling principles" should be powerful enough to model physically heterogeneous interfaces, handle non-matched discrete nodal distributions, and guide the rational choice of admissible discretization function spaces along the partition boundaries.

The present paper addresses the construction of such principles for structural mechanics models. The main novel features are: (i) the use of separately varied partition-frame displacements and Lagrange multipliers to link arbitrarily connected meshes of mechanical finite elements, and (ii) the explicit separation of rigid-body and deformational motions so that the solvability conditions for floating partitions are automatically provided as part of the formulation.

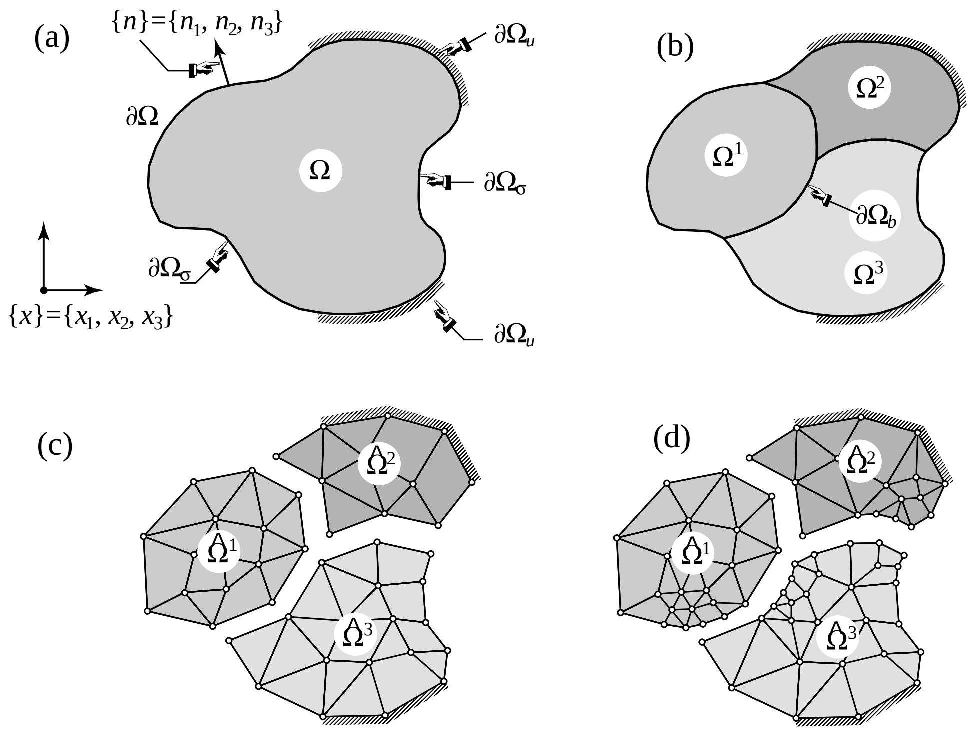

Figure 1. (a) A domain Ω with boundary $\partial\Omega = \partial\Omega_\sigma \cup \partial\Omega_u$; (b): partition into three subdomains: Ω^1, Ω^2 and Ω^3 by cutting it through interface $\partial\Omega_b$. Two FEM discretizations of (b): (c) matching submeshes; (d) nonmatching submeshes. Superposed hats distinguish discrete versions.

2. VARIATIONAL PRINCIPLES AND LAGRANGE MULTIPLIERS

There exist a rich body of literature on the variational principles in structural mechanics. Survey articles and book chapters oriented to such applications may be found in Argyris and Kelsey,[1] Fraeijs de Veubeke,[2] Washizu,[3] Pian and Tong,[4] Pian,[5] Atluri,[6] Oden and Reddy,[7] Reddy,[8] Hughes,[9] Zienkiewicz and Taylor,[10] and Felippa.[11]

Most of these principles were developed with finite element models in mind. In particular, developments of hybrid and mixed principles since the mid-1960s, pioneered by Pian[12] and Herrmann,[13] were largely driven by the goal of relaxing displacement continuity requirements so as to formulate better performing elements. Those principles introduce additional independent variables which, as pointed out by Fraeijs de Veubeke in several important articles[2,14,15] may be viewed as an application of the method of Lagrange multiplier fields. Those fields are adjoined through standard techniques such as Friedrichs' dislocation potentials[16] or Legendre transforms.[17] In hybrid principles the multipliers may be physically interpreted as internal fields such as stresses, pressures, tractions or strains. Upon discretization the associated variables are eliminated at the element level to produce elements with the standard external displacement degrees of freedom.

It is recalled that Lagrange's original motivation for what he called the "method of indeterminate coefficients" was to derive the equilibrium equations of a system of constrained rigid bodies, or "particles" in Newtonian mechanics parlance. To this end, Lagrange treated the problem "as if all bodies are entirely free" and formulated the virtual work by summing up the contributions of "entirely free" individual bodies. He then identified the "equations of condition" [in modern terminology, the constraint equations] among the kinematic differential variables. Once identified, each constraint equation was multiplied by an indeterminate coefficient and added to the virtual work of the free bodies to yield the total virtual work of the system. He states: "the sum of all the terms which are multiplied by the same differential [same variation in modern usage] are equated to zero, which will give as many particular solutions as there are differentials. . . . These equations, being then rid of the indeterminate coefficients by elimination, will provide all of the conditions necessary for equilibrium." See Lagrange,[18] Lanczos[19] or Dugas.[20] Hence the notion of eventual elimination of multipliers has strong historical roots.

The partitioning scheme considered here *retains* Lagrange multipliers on interfaces rather than eliminating them. It represents a continuum generalization of the localized Lagrange multiplier (LLM) method, presented by Park and Felippa[21] for discrete mechanical systems whose interface freedoms match. For matching meshes one advantage of the LLM method over the classical multiplier method is the treatment of the so-called cross points, namely nodes whose freedoms are shared by more than two submeshes. The LLM method yields a unique set of constraint conditions. That appealing simplicity breaks down for nonmatching meshes. To handle those complications it is convenient to move to a continuum level framework, and treat multipliers as interface fields to be appropriately interpolated. Those interpolation functions cannot be arbitrarily chosen, but must satisfy Fraeijs de Veubeke's limitation principle.[2] The LLM for matched meshes is recovered as a particular case, in which the interface multipliers are interpolated by node-collocated delta functions.

When multipliers are retained as interface connectors the "floating partition" problem arises. In the standard displacement formulation of finite elements the rigid body modes (RBM) are implicitly embodied in the strain-displacement equations. Upon assembly and application of support conditions the discrete stiffness equations are rid of RBMs (except in special problems, such as free-free dynamics). In multiplier-connected systems the RBMs of each partition must be explicitly identified and be in self-equilibrium under rigid-body motions. This self-equilibrium condition was apparently first stated by Fraeijs de Veubeke[22] as providing the fundamental solvability conditions for disconnected elements. It has played a pivotal role in the development of the Finite Element Tearing and Interconnecting (FETI) method developed by Farhat, Roux and coworkers[23–26] for parallel computation of structural mechanics problems. These precursors to the present formulation are discussed in Section 6.

3. CONTINUUM VARIATIONAL FORMULATION

In a 1975 article, Atluri[6] presented two hybrid functionals, labeled HWM1 and HWM2 (for "Hu-Washizu Modified"), which collectively extend the Hu-Washizu (HW) principle to accommodate internal interfaces. The five-field functional HMW1 extends HW with the interface discontinuity term proposed by Prager,[27] which links interface displacements through a single Lagrange multiplier field. The six-field functional HWM2 includes independently varied boundary displacements weakly linked to interior displacements by subdomain-localized Lagrange multipliers fields. This approach is relevant to the present development.

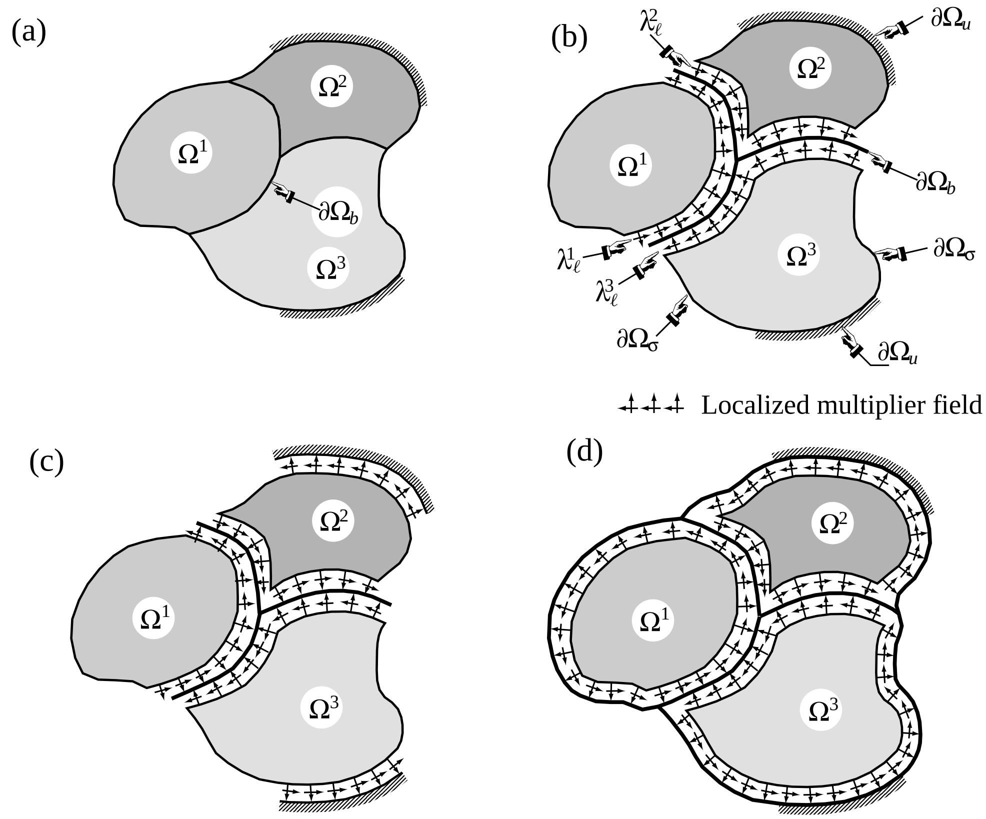

Figure 2. Interface treatment used in constructing several functionals. (a) The domain of Figure 1(a) divided into three subdomain partitions; (b) Functional Π_{HWM2}: linkup by localized Lagrange multipliers and partition-frame displacements; (c) Functional Π_{PEM2}: the multiplier fields are extended to include prescribed-displacement portions $\partial\Omega_u$; (d) Functional Π_{UFF}: the multiplier fields are extended to cover all boundaries, whether internal or external.

3.1 The HMW2 Functional

Key ingredients of HWM2 are illustrated in Figures 1 and 2. The elastic body of Figure 1(a) occupies domain Ω, referred to a Cartesian system x_i. The boundary $\partial\Omega$ has exterior normal n_i. The domain is partitioned into three subdomains Ω_1, Ω_2 and Ω_3 as depicted in Figure 2(a). An internal boundary $\partial\Omega_b$ called a *partition frame*, is placed as shown in Figure 2(b). The displacements of $\partial\Omega_b$ are to be varied independently from those of the subdomains. The partition frame is "glued" to the adjacent subdomains by Lagrange multiplier fields λ_ℓ. These multipliers are said to be *localized* because they are associated with subdomains.

The interior fields of subdomain Ω^m, considered as an isolated entity, are: displacements u_i^m, strain ϵ_{ij}^m, stress σ_{ij}^m and prescribed body force $\bar{f}_i^m$. Its boundary $\partial\Omega^m$ can be generally decomposed into $\partial\Omega_u^m$, $\partial\Omega_\sigma^m$ and $\partial\Omega_b^m$. $\partial\Omega_u^m$ and $\partial\Omega_\sigma^m$ are portions of $\partial\Omega^m$ where displacements $\bar{u}_i$ and tractions $\bar{t}_i$, respectively, are prescribed. $\partial\Omega_b^m$ is the interface with other subdomains, over which the Lagrange multiplier field $\lambda_{\ell i}^m$ has the role of surface traction. Subdomain linking is done through the displacement u_{bi} of the partition frame $\partial\Omega_b$. The strain energy density and symmetric displacement gradients are denoted by

$$\mathcal{U}(\epsilon_{ij}) = \tfrac{1}{2} E_{ijkl}\, \epsilon_{ij}\, \epsilon_{kl}, \quad u_{(i,j)} = \tfrac{1}{2}(u_{i,j} + u_{j,i}), \tag{1}$$

respectively, in which E_{ijkl} are the elastic moduli, commas denote partial derivatives, and the summation convention is in effect. With these ingredients in place, the HWM2 functional for linear elastostatics can be presented as a sum of subdomain contributions:

$$\Pi_{\rm HWM2}(u_i, \epsilon_{ij}, \sigma_{ij}, t_i, \lambda_{\ell i}, u_{bi}) \;=\; \Pi_{\rm HW} - \pi_u \;=\; \sum_m \Pi^m_{\rm HW} - \sum_m \pi^m_u, \tag{2}$$

in which

$$\begin{aligned}
\Pi^m_{\rm HW} &= \int_{\partial\Omega^m} \left[\mathcal{U}(\epsilon^m_{ij}) + \sigma^m_{ij}(u^m_{(i,j)} - \epsilon^m_{ij}) - u^m_i\, \bar{f}^m_i \,\right] d\Omega - \int_{\partial\Omega^m_\sigma} u^m_i\, \bar{t}^m_i\, dS - \int_{\partial\Omega^m_u} t^m_i\, (u^m_i - \bar{u}^m_i)\, dS, \\
\pi^m_u &= \int_{\partial\Omega^m_b} \lambda^m_{\ell i}(u^m_i - u_{bi})\, dS.
\end{aligned} \tag{3}$$

The sum over m extends from 1 to the number of subdomains N_s. For the boundary integrals dS is used to denote the boundary differential instead of the clumsier $d\partial\Omega$. Note that $\Pi^m_{\rm HW}$, called the *interior functional* for obvious reasons, is fully subdomain localized since all entities have superscript m. The only interpartition connection is through u_{bi} in π^m_u, which is called an *interface potential* or *dislocation potential* in continuum mechanics. The sum of the π^m_u results in the integral being carried out twice on each interface, once on each side of $\partial\Omega_b$, as is typical of hybrid functionals. If the compatibility condition $u^m_i = u_{bi}$ is enforced *a priori*, π_u drops out and the ordinary Hu-Washizu functional $\Pi_{\rm HW}$ results. [The HW functional is expressable in two forms, which can be transformed from from one to another through integration by parts].

Atluri[6] shows that the stationarity condition $\delta\Pi_{\rm HWM2} = 0$ yields: (i) the elasticity field equations $\epsilon_{ij} = u_{(i,j)}$, $\sigma_{ij} = E_{ijkl}\epsilon_{kl}$ and $\sigma_{ij,j} + \bar{f}_i = 0$ in Ω as Euler equations; (ii) the displacement boundary condition $u_i = \bar{u}_i$ on $\partial\Omega_u$ and the traction boundary condition $\bar{t}_i = \sigma_{ij}n_j$ on $\partial\Omega_\sigma$ as natural boundary conditions; (iii) the interface compatibility $u_i = u_{bi}$ and traction equilibrium $\lambda_{\ell i} = t_i$ on $\partial\Omega_b$ as interface continuity conditions.

The original objective for (3), as well as specializations thereof, was construction of finite elements. If the interface $\partial\Omega_b$ surrounds each element, each subdomain collapses to an individual element. All interior fields: u^m_i, ϵ^m_{ij} and σ^m_{ij}, as well as the multiplier field $\lambda^m_{\ell i}$, are eliminated at the element level, leaving only the boundary frame displacement u_{bi} as primary unknown. This is the standard technique for constructing hybrid models. The resulting elements can be processed by FEM programs as if they were ordinary displacement models. For use of (3) in partitioned analysis, however, it will be found convenient to retain all boundary frame fields in the discrete equations.

3.2 Simplifications

We are primarily interested in the treatment of interface conditions rather than constructing new elements. Hence we begin by simplifying $\Pi_{\rm HWM2}$ in two respects:

1. The relations $\epsilon_{ij} = u_{(i,j)}$ and $\sigma_{ij} = E_{ijkl}u_{(k,l)}$ in Ω are imposed *a priori*. This eliminates ϵ_{ij} and σ_{ij} as independently varied fields, and reduces the interior functional to the Potential Energy (PE) functional.
2. Prescribed displacement portions $\partial\Omega_u$ of $\partial\Omega$ are treated in the same way as $\partial\Omega_b$. The traction field t_i on those portions is identified with the multiplier field $\lambda_{\ell i}$, as illustrated in Figure 2(c). This modification allows processing all subdomains as free-free (i.e., possessing a full set of rigid-body modes), which simplifies the computer implementation.

These changes reduce (2) to a modified form of the Potential Energy functional:

$$\Pi_{\rm PEM2}(u_i, \lambda_{\ell i}, u_{bi}) \;=\; \Pi_{\rm PE} - \pi_u \;=\; \sum_m \Pi^m_{\rm PE} - \sum_m \pi^m_u, \tag{4}$$

in which

$$\begin{aligned} \Pi^m_{\rm PE} &= \int_{\Omega^m} \left[\mathcal{U}(u^m_i) - u^m_i\, \bar f^m_i\,\right] d\Omega - \int_{\partial\Omega^m_\sigma} u^m_i\, \bar t^m_i\, dS, \\ \pi^m_u &= \int_{\partial\Omega^m_b \cup \partial\Omega^m_u} \lambda^m_{\ell i}(u^m_i - u_{bi})\, dS. \end{aligned} \tag{5}$$

To redefine π_u, the frame displacements u_{bi} are formally extended so that $u_{bi} = \bar u_i$ on $\partial\Omega_u$. The functional labeled $\Pi_{\rm HD2}$ by Atluri[6] is essentially $\Pi_{\rm PEM2}$, except for keeping the original integral over $\partial\Omega_u$ in the interior functional. That hybrid functional was originally proposed by Tong.[28]

A related functional is the one that governs the Unscaled Free Formulation[29,30] of finite elements:

$$\Pi_{\rm UFF}(u_i, t_i, u_{bi}) = \sum_m \left[\int_{\Omega^m} \left[\mathcal{U}(u^m_i) - u^m_i\, \bar f^m_i\,\right] d\Omega - \int_{\partial\Omega^m_\sigma} u^m_{bi}\, \bar t^m_i dS - \int_{\partial\Omega^m} t^m_i(u^m_i - u_{bi})\, dS\right]. \tag{6}$$

The interface integral of $\Pi_{\rm UFF}$ extends over the *complete boundary* of each subdomain: $\partial\Omega^m : \partial\Omega^m_\sigma \cup \partial\Omega^m_u \cup \partial\Omega^m_b$, as illustrated in Figure 2(d). This form can be obtained from (4) by extending u_{bi} and $\lambda_{\ell i}$ to $\partial\Omega_\sigma$, adding and subtracting $\int_{\partial\Omega_\sigma} \lambda_{\ell i}(u_i - u_{bi})\, dS$ and renaming $\lambda_{\ell i} \to t_i$. Note that the $\partial\Omega^m_\sigma$ term in (6) involves u_{bi} and not u^m_i. This treatment of traction boundary conditions is more convenient for individual element formulations because in that case the internal displacements u^m_i are eliminated at the element level. The Scaled FF functional contains a free parameter in the interior component that interpolates between the Potential Energy and Hellinger-Reissner forms.[30]

3.3 Displacement Decomposition

For several applications of partitioned analysis, notably inverse problems and parallel solution, it is convenient to explicitly separate the rigid body modes in the governing equation of floating subdomains. Following de Veubeke[22] this is done by decomposing of total displacements into deformational and rigid-body components:

$$u_i(x_k) = d_i(x_k) + r_i(x_k). \tag{7}$$

Since $u_{(i,j)} = d_{(i,j)}$ the strain energy density $\mathcal{U}$ becomes function of the deformational displacements d_i only: $\mathcal{U}(d_i) = \frac{1}{2} E_{ijkl}\, d_{(i,j)}\, d_{(k,l)}$. Inserting (7) into (4) we obtain the four-field functional

$$\tilde\Pi_{\rm PEM2}(d_i, r_i, \lambda_{\ell i}, u_{bi}) \;=\; \tilde\Pi_{\rm PE} - \tilde\pi_u \;=\; \sum_m \tilde\Pi^m_{\rm PE} - \sum_m \tilde\pi^m_u, \tag{8}$$

in which

$$\begin{aligned} \tilde\Pi^m_{\rm PE} &= \int_{\Omega^m} \left[\mathcal{U}(d^m_i) - (d^m_i + r^m_i)\, \bar f^m_i\,\right] d\Omega - \int_{\partial\Omega^m_\sigma} (d^m_i + r^m_i)\, \bar t^m_i\, dS \\ \tilde\pi^m_u &= \int_{\partial\Omega^m_b} \lambda^m_{\ell i}(d^m_i + r^m_i - u_{bi})\, dS \end{aligned} \tag{9}$$

3.4 Deformation-RBM Orthogonality Condition

Given a subdomain displacement field u_i^m, the decomposition (7) is unique if the following orthogonality condition is imposed:

$$\int_{\Omega^m} d_i^m\, r_i^m\, d\Omega = \int_{\Omega^m} (u_i^m - r_i^m)\, r_i^m\, d\Omega = 0 \tag{10}$$

This can be shown as follows. Over each subdomain the rigid body displacements can be expressed as

$$r_i^m = R_{ij}^m\, \alpha_j^m, \tag{11}$$

where α_j^m are subdomain rigid body mode (RBM) amplitudes and R_{ij}^m are entries of a dimensionless full-rank matrix $\mathbf{R}^m$ whose columns span the RBMs. The entries of $\mathbf{R}^m$ are at most linear in the coordinates x_i. $\mathbf{R}^m$ is formed by selecting a linearly independent RBM basis for its columns, followed by orthonormalization: $\int_{\Omega^m} R_{ji}^m R_{ik}^m = V^m\, \delta_{jk}$, in which δ_{jk} is the Kronecker delta and $V^m = \int_{\Omega^m} d\Omega$ is the subdomain volume (area, length). Substitution into the second of (10) yields

$$\left(\int_{\Omega^m} u_i^m\, R_{ij}^m\, d\Omega - \alpha_k^m \int_{\Omega^m} R_{ki}^m R_{ij}^m\, d\Omega \right) \alpha_j^m = \left(P_j^m - V^m \alpha_j^m \right) \alpha_j^m = 0, \tag{12}$$

where $P_j^m = \int_{\Omega^m} u_i^m R_{ij}^m\, d\Omega$. The nontrivial solution of (12) is obtained by taking $\alpha_j^m = P_j^m / V^m$. We observe that the RBM amplitude α_j^m is merely the projection of the displacement u_i^m on the j^{th} rigid body mode R_{ij}^m. If $\mathbf{R}^m$ is not orthonormalized the inverse of a weighting matrix appears in (12).

3.5 Stationarity Conditions: Static Case

Varying $\Pi_{\rm PEM2}$ in the static case yields the weak (Galerkin) form

$$\delta\Pi_{\rm PEM2} = \sum_m \left\{ G_{di}^m\, \delta d_i^m + G_{\alpha i}^m\, \delta\alpha_i^m + G_{\lambda\ell i}^m\, \delta\lambda_{\ell i}^m + G_{ubi}^m\, \delta u_{bi} \right\}, \tag{13}$$

in which account is taking of (11) to express $\delta r_j^m = R_{ji}^m \delta\alpha_i^m$. The subdomain variational coefficients are

$$\begin{aligned}
G_{di}^m &= \int_{\Omega^m} p_i^m\, d\Omega - \int_{\Omega^m} \bar{f}_i^m\, d\Omega - \int_{\partial\Omega_\sigma^m} \bar{t}_i^m\, dS - \int_{\partial\Omega_b^m} \lambda_{\ell i}^m\, dS,\\
G_{\alpha i}^m &= -\int_{\Omega^m} \bar{f}_j^m R_{ij}^m\, d\Omega - \int_{\partial\Omega_\sigma^m} \bar{t}_j^m\, R_{ij}^m\, dS - \int_{\partial\Omega_b^m} \lambda_{\ell j}^m\, R_{ij}^m\, dS,\\
G_{\lambda\ell i}^m &= -\int_{\partial\Omega_b^m} [d_i^m + r_i^m - u_{bi}]\, dS,\\
G_{ubi}^m &= -\int_{\partial\Omega_b^m} \lambda_{\ell i}^m dS.
\end{aligned} \tag{14}$$

In the first of (14), p_i^m is the internal force density that results from the variation of the internal energy density: $\delta\mathcal{U}^m = p_i^m\, \delta d_i^m$. Setting the variation (13) to zero provides weak forms of deformational equilibrium, rigid-body equilibrium, interface compatibility (including prescribed displacements) and interface equilibrium (Newton's third law at subdomain boundaries) conditions, respectively. The first two are *localized* at the subdomain level. The only connection between subdomains is done through the last two conditions, which bring in the partition frame displacements u_{bi}.

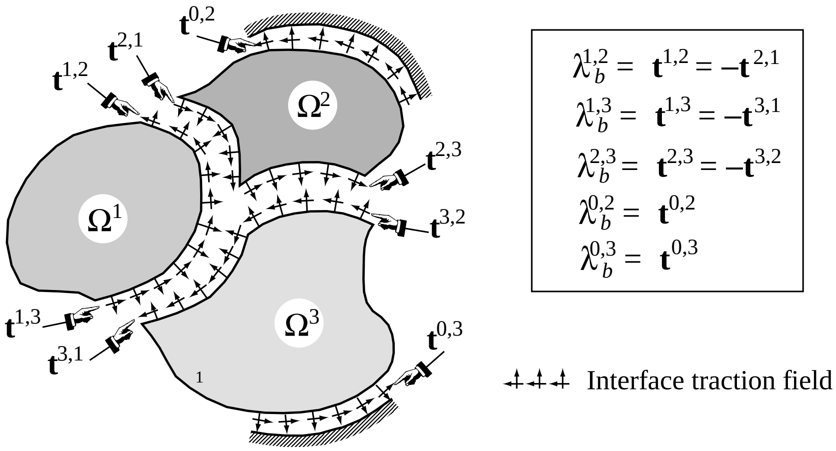

Figure 3. Direct subdomain connection using global Lagrange multipliers.

3.6 Stationarity Conditions: Dynamic Case

Functional (10) can be formally extended to dynamic problems through the substitution of $\bar{f}_i$ by the D'Alembert's force

$$f_i = \bar{f}_i - \rho(\ddot{d}_i + \ddot{r}_i) \tag{15}$$

With this replacement $\delta\tilde{\Pi}_{\rm PEM2} = 0$ is a restricted variational principle in which time is to be held frozen on variation. We note that, if desired, it can be transformed to a Hamiltonian principle through integration by parts of the kinetic energy terms.

The substitution (15) produces kinetic energy density terms in the four combinations $\rho r_i \ddot{r}_i$, $\rho d_i \ddot{r}_i$, $\rho \ddot{d}_i r_i$ and $\rho r_i \ddot{r}_i$. If ρ is constant, enforcing the orthogonality condition (10) makes the cross-coupling terms $d_i \ddot{r}_i$ and $\ddot{d}_i r_i$ vanish on integration over Ω^m. If ρ is not constant over the subdomain, however, (10) must be modified with the mass density as weight function:

$$\int_{\Omega^m} \rho^m d_i^m\, r_i^m \, d\Omega = \int_{\Omega^m} \rho^m (u_i^m - r_i^m)\, r_i^m \, d\Omega = 0. \tag{16}$$

This results in simple modifications to the integrals of (12). Assuming this "mass orthogonality" is enforced, the restricted variation (with frozen time) leads again to the weak form (13), in which the first two coefficients are augmented with acceleration terms:

$$\begin{aligned} G_{di}^m &= \int_{\Omega^m} p_i^m \, d\Omega - \int_{\Omega^m} (\bar{f}_i^m - \rho^m \, \ddot{d}_i^m)\, d\Omega - \int_{\partial\Omega_\sigma^m} \bar{t}_i^m \, dS - \int_{\partial\Omega_b^m} \lambda_{\ell i}^m \, dS, \\ G_{\alpha i}^m &= - \int_{\Omega^m} (\bar{f}_j^m R_{ij}^m - \rho^m \, R_{ij}^m \, \ddot{\alpha}_j^m)\, d\Omega - \int_{\partial\Omega_\sigma^m} \bar{t}_j^m \, R_{ij}^m \, dS - \int_{\partial\Omega_b^m} \lambda_{\ell i}^m \, R_{ij}^m \, dS. \end{aligned} \tag{17}$$

3.7 Connection Through Global Lagrange Multipliers

As noted in the historical remarks of Section 2, in the classical method of Lagrange multipliers developed originally for particle and celestial mechanics, constrained bodies are directly connected by interaction forces. The equivalent technique for partitioned analysis is illustrated in Figure 3. The partition frame $\partial\Omega_b$ that effectively localizes the Lagrange multipliers is omitted. Compatibility of boundary displacements of two connected subdomains, m and n, is enforced by traction fields $t_i^{m,n}$ and $t_i^{n,m}$, which satisfy Newton's third law $t_i^{m,n} + t_i^{n,m} = 0$. To avoid carrying over two sets of tractions, a *from-to sign convention* must be established. For each pair $\{m, n\}$ of linked subdomains, we chose the traction flow as positive from m to n if $m < n$. The global multiplier field $\lambda_{bi}^{m,n}$ is defined as $\lambda_{bi}^{m,n} = t_i^{m,n} = -t_i^{n,m}$ for $m < n$. This rule can be subsumed into one equation using an alternator symbol:

$$\lambda_{bi}^{m,n} = c^{m,n}\, t_i^{m,n}, \quad \text{in which} \quad c^{m,n} = \begin{cases} 0 & \text{if } m = n \text{ or } \{m, n\} \text{ are not connected,} \\ +1 & \text{if } m < n, \\ -1 & \text{if } m > n. \end{cases} \tag{18}$$

The notation is extended to include the prescribed displacement portions by conventionally identifying the ground as subdomain zero (see Figure 3). Hence m ranges from 0 to the number of subdomains N_s.

The variational form of this technique is based on the hybrid functional

$$\Pi_{\text{PEM1}}(u_i, \lambda_{bi}) = \Pi_{\text{PE}} - \pi_\lambda, \tag{19}$$

where Π_{PE} is the same as in Π_{PEM2}, and

$$\pi_\lambda = \int_{\partial\Omega_b} \lambda_{bi}\, u_i\, dS = \sum_{m=0}^{N_s} \sum_{n=1}^{N_s} \int_{\partial\Omega_b^{m,n}} c^{m,n} t_i^{m,n}\, u_i^m\, dS. \tag{20}$$

This interface potential was first proposed by Prager[27] to treat internal physical discontinuities. If coupled with Π_{HW}, a functional similar to Π_{HWM1} of Atluri[6] results but for the different treatment of $\partial\Omega_u$. Inserting the decomposition $u_i = d_i + r_i$ into Π_{PEM1} yields

$$\tilde{\Pi}_{\text{PEM1}}(r_i, d_i, \lambda_{bi}) = \tilde{\Pi}_{\text{PE}} + \tilde{\pi}_\lambda, \tag{21}$$

where

$$\tilde{\pi}_\lambda = \int_{\partial\Omega_b} \lambda_{bi}\, (d_i + r_i)\, dS = \sum_{m=0}^{N_s} \sum_{n=1}^{N_s} \int_{\partial\Omega_b^{m,n}} c^{m,n} t_i^{m,n} (d_i^m + r_i^m)\, dS \tag{22}$$

The variation of $\tilde{\Pi}_{\text{PEM1}}$ in the static case yields the weak form

$$\delta\tilde{\Pi}_{\text{PEM1}} = \sum_m \left\{ G_{di}^m\, \delta d_i + G_{\alpha i}^m\, \delta\alpha_i^m \right\} + \sum_m \sum_n G_{\lambda i}^{m,n}\, \delta\lambda_{bi} \tag{23}$$

where

$$\begin{aligned} G_{di}^m &= \int_{\Omega^m} p_i^m\, d\Omega - \int_{\Omega^m} \bar{f}_i^m\, d\Omega - \int_{\partial\Omega_\sigma^m} \bar{t}_i^m\, dS - \int_{\partial\Omega_b^m} \lambda_{bi}\, dS, \\ G_{\alpha i}^m &= -\int_{\Omega^m} \bar{f}_j^m R_{ij}^m\, d\Omega - \int_{\partial\Omega_\sigma^m} \bar{t}_j^m\, R_{ij}^m\, dS - \int_{\partial\Omega_b^m} \lambda_{bj}\, R_{ij}^m\, dS, \\ G_{\lambda i}^{m,n} &= -\int_{\partial\Omega_b^{m,n}} c^{m,n} (d_i^m + r_i^m)\, dS, \end{aligned} \tag{24}$$

Generalization to the dynamic case can be carried out as in the case of $\tilde{\Pi}_{\text{PEM2}}$.

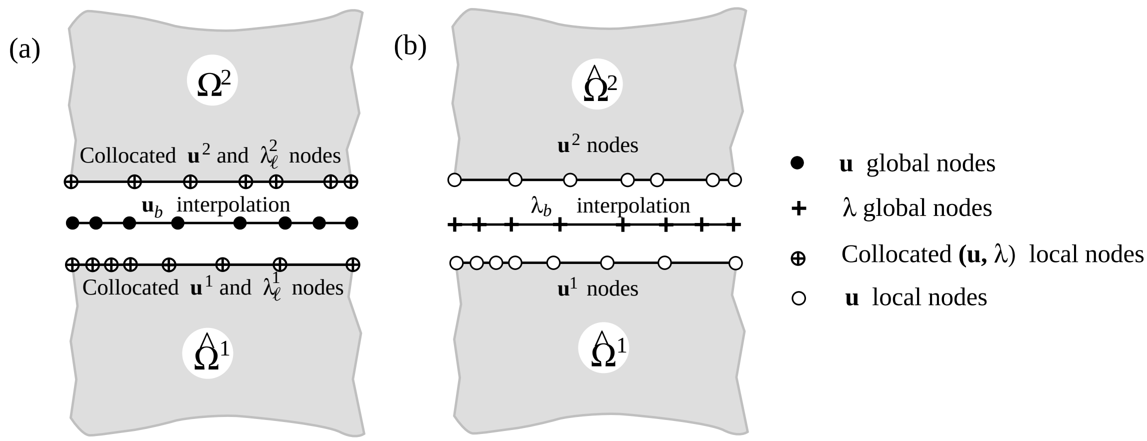

Figure 4. Two connection schemes for nonmatched mesh interfaces: (a) connection by global displacements and node-force-collocated local multipliers; (b) connection by global multipliers.

4. TREATMENT OF NONMATCHING MESHES

As noted in the Introduction, nonmatching meshes can arise from a variety of sources: separately constructed discretizations, localized refinement, global-local analysis and coupled-field problems. The functionals (4) and (8) provide adequate tools to treat nonmatching meshes of mechanical finite elements. This section discusses aspects of the discretization procedure associated with the use of Lagrange multipliers. It should be noted that primal techniques that do not use multipliers, such as the "mortar method" of Bernardi, Maday and Patera,[31] have been recently developed to couple nonmatching meshes. Such techniques are appropriate when master and slaves interfaces can be readily identified; for example a fine mesh linked to a coarse one as is common in global-local analysis.

For definiteness the discussion refers to the case illustrated in Figure 4. Upon discretization the nodes on the partition frame $\partial\Omega_b$ match neither with those on subdomain Ω^1 nor subdomain Ω^2. The two interface methods depicted there correspond to the functionals $\Pi_{\rm PEM2}$ and $\Pi_{\rm PEM1}$, respectively. Throughout this Section the displacement field is kept as u_i, without decomposing into r_i and d_i, to clarify the exposition. The more general case is dealt with in Section 5.

The continuum interface potential for the localized functional (5) is given by

$$\pi_u(u_i^1, u_i^2, \lambda_{\ell i}^1, \lambda_{\ell i}^2, u_{bi}) = \int_{\partial\Omega^1} \lambda_{\ell i}^1\, u_i^1\, dS + \int_{\partial\Omega^2} \lambda_{\ell i}^2\, u_i^2\, dS - \int_{\partial\Omega_b^1} \lambda_{\ell i}^1\, u_{bi}\, dS - \int_{\partial\Omega_b^2} \lambda_{\ell i}^2\, u_{bi}\, dS \tag{25}$$

In the above expressions, $\partial\Omega_b^1$ denotes the projection of the attributes on $\partial\Omega^1$ onto $\partial\Omega_b$, and similarly for $\partial\Omega_b^2$.

The continuum interface potential for the global functional (18) is given by

$$\pi_\lambda(u_i^1, u_i^2, \lambda_{bi}) = \int_{\partial\Omega_b^1} \lambda_{bi}\, u_i^1\, dS\, - \int_{\partial\Omega_b^2} \lambda_{bi}\, u_i^2\, dS \tag{26}$$

4.1 Discretization by Localized Multipliers

The FEM interpolations assumed for the case of Figure 4(a) are

$$\{u^1\} = \mathbf{N}_u^1 \mathbf{u}^1, \quad \{u^2\} = \mathbf{N}_u^2 \mathbf{u}^2, \quad \{\lambda^1\} = \mathbf{N}_\lambda^1 \boldsymbol{\lambda}^1, \quad \{\lambda^2\} = \mathbf{N}_\lambda^2 \boldsymbol{\lambda}^2, \quad \{u_b\} = \mathbf{N}_u^b \, \mathbf{u}_b. \tag{27}$$

where $\mathbf{N}_u^1$, for example, collects the shape functions of the interface displacement $\{u^1\}$. If the example of Figure 4 corresponds to plane stress, $\mathbf{N}_u^1$ would be a 2×16 matrix, since there are then two displacement components ($i = 1, 2$) and eight nodes on the Ω^1 interface; matrices $\mathbf{N}_u^2$, $\mathbf{N}_\lambda^1$, $\mathbf{N}_\lambda^2$ and $\mathbf{N}_u^b$ would be dimensioned 2×14, 2×16, 2×14 and 2×16, respectively.

Substituting these interpolations into (25) the discrete version results:

$$\hat{\pi}_u(\mathbf{u}^1, \mathbf{u}^2, \boldsymbol{\lambda}^1, \boldsymbol{\lambda}^2, \mathbf{u}_b) = \left(\boldsymbol{\lambda}^1\right)^T \left(\mathbf{C}_1 \, \mathbf{u}^1 - \mathbf{C}_{1b} \, \mathbf{u}_b\right) + \left(\boldsymbol{\lambda}^2\right)^T \left(\mathbf{C}_2 \, \mathbf{u}^2 - \mathbf{C}_{2b} \, \mathbf{u}_b\right), \tag{28}$$

in which the $\mathbf{C}$ are connection matrices (also called constraint matrices):

$$\mathbf{C}_k = \int_{\partial\Omega^k} (\mathbf{N}_\lambda^k)^T \mathbf{N}_u^k \, dS, \quad \mathbf{C}_{kb} = \int_{\partial\Omega_b^k} (\mathbf{N}_\lambda^k)^T \mathbf{N}_u^b \, dS, \quad k = 1, 2. \tag{29}$$

The simplest choice for multiplier interpolation is *node force collocation*, in which the multipliers are simply point (concentrated) forces at multiplier nodes that coincide with the local displacement nodes. This choice is that depicted in Figure 4(a) by merging cross and circle symbols. Matrices $\mathbf{N}_\lambda^1$ and $\mathbf{N}_\lambda^2$ consist of delta functions collocated at the subdomain mesh nodes. If so, $\mathbf{C}_1$ and $\mathbf{C}_2$ reduce to identity matrices whereas the entries of $\mathbf{C}_{1b}$ and $\mathbf{C}_{2b}$ are obtained simply by evaluating $\mathbf{N}_u^b$ at interface nodes. Furthermore the interface force vector associated with the multiplier nodal values is simply

$$\mathbf{f}_b = \begin{bmatrix} \dfrac{\partial \hat{\pi}_u}{\partial \mathbf{u}^1} \\ \dfrac{\partial \hat{\pi}_u}{\partial \mathbf{u}^2} \end{bmatrix} = \begin{bmatrix} \boldsymbol{\lambda}^1 \\ \boldsymbol{\lambda}^2 \end{bmatrix}. \tag{30}$$

Consequently full domain discretization accuracy is preserved. Another advantage of the node-force-collocated multiplier discretization is the fact that $\mathbf{N}_u^1$ and $\mathbf{N}_u^2$ do not appear in the connection matrices. Hence the implementor of a partitioned analysis program need not know the types of finite element that are being linked. This feature helps software modularity.

If collocation is adopted, there still remains the problem of interpolating the frame displacements. As a general guideline, if the number of interface nodes on subdomains Ω^1 and Ω^2 is n_1 and n_2, respectively, the number of global displacement nodes, marked by a dark circle in Figure 4(a), should be at least $\max(n_1, n_2)$. This rule does not tell, however, how those nodes should be placed. This is the subject of current research.

If the meshes match, that is, when all nodes are collocated and the multipliers are node forces, the connection matrices reduce to Boolean matrices with 0 or 1 entries.

4.2 Discretization by Globalized Multipliers

For the globalized multiplier case the FEM interpolation is

$$\{u^1\} = \mathbf{N}_u^1 \, \mathbf{u}^1, \quad \{u^2\} = \mathbf{N}_u^2 \, \mathbf{u}^2, \quad \{\lambda_b\} = \mathbf{N}_\lambda^b \, \mathbf{u}_i. \tag{31}$$

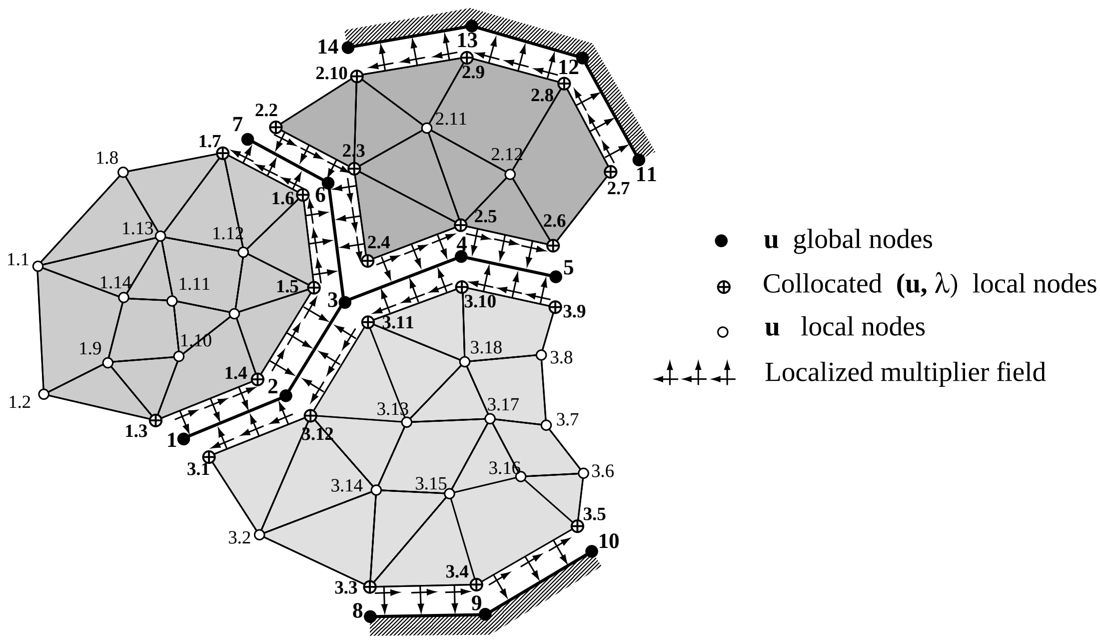

Figure 5. Localized-multiplier FEM discretization of example domain of Figure 1(c). Matched submeshes shown for simplicity. Three node types are identified by indicated symbols. Prescribed displacement portions of the boundary are treated as internal interfaces. Global nodes conventionally belong to subdomain zero. Hence node numbers 1,2,. . . could have also been identified 0.1, 0.2, . . ., should that simplify the implementation.

where $\mathbf{N}_\lambda^{1,2}$ is constructed from the multiplier nodes marked by a cross in Figure 4(b). The rules for selecting such nodes are more delicate than in the previous case. The discretized interface functional is

$$\hat{\pi}_\lambda(\mathbf{u}^1, \mathbf{u}^2, \boldsymbol{\lambda}_b) = \left(\boldsymbol{\lambda}_b\right)^T \left(\mathbf{C}_{\lambda 1}\, \mathbf{u}^1 - \mathbf{C}_{\lambda 2}\, \mathbf{u}^2\right) \tag{32}$$

in which

$$\mathbf{C}_{\lambda 1} = \int_{\partial\Omega_b} (\mathbf{N}_\lambda^b)^T\, \mathbf{N}_u^1\, dS, \quad \mathbf{C}_{\lambda 2} = \int_{\partial\Omega_b} (\mathbf{N}_\lambda^b)^T\, \mathbf{N}_u^2\, dS. \tag{33}$$

Again, should λ_b be defined by point forces at multiplier nodes the connection matrices can be simply constructed by evaluating $\mathbf{N}_u^1$ and $\mathbf{N}_u^2$ at the multiplier nodes. The displacement interpolation, however, would depend on the type of element adjacent to the interface. This hinders software modularity.

The interface force vector associated with the multiplier nodal values is

$$\mathbf{f}_b = \begin{bmatrix} \dfrac{\partial \hat{\pi}_\lambda}{\partial \mathbf{u}^1} \\ \dfrac{\partial \hat{\pi}_\lambda}{\partial \mathbf{u}^2} \end{bmatrix} = \begin{bmatrix} \mathbf{C}_{\lambda 1}\, \boldsymbol{\lambda}^1 \\ -\mathbf{C}_{\lambda 2}\, \boldsymbol{\lambda}^2 \end{bmatrix} \tag{34}$$

On studying the expressions (30) and (34) for the interface forces, we find that in the former there emerges a least-squares projection operator that plays the role of filtering out the boundary frame modes. This property enforces Newton's action-reaction law in a least-square sense. On the other hand, there is no *a priori* guarantee that the law would be satisfied by (34). Preliminary numerical experiments corroborate these remarks.

If the meshes match and node force collocation is used for λ_b, the connection matrices become incident matrices, with entries ± 1 or 0. Note that these are no longer Boolean matrices.

5. FEM DISCRETIZATION

We now pass to consider the displacement-based FEM discretization of the $\Pi_{\rm PEM2}$ functional. A typical configuration of the resulting discretization is illustrated in Figure 5. Although a matched mesh is shown for visualization convenience, the development that follows is valid for nonmatching meshes. Three types of node points illustrated in Figure 5 should be distinguished:

1. Global interface nodes, or $\mathbf{u}_b$ nodes, which define the interpolation on $\partial\Omega_b$ and $\partial\Omega_u$. These are numbered 1 through 14 in Figure 5. Conventionally these belong to subdomain zero.
2. Local interface nodes or $(\mathbf{u}, \lambda)$ nodes, which for matched meshes are paired with the global nodes on $\partial\Omega_b$ and $\partial\Omega_u$. For example, local nodes 2.5 and 3.10 are paired to global node 4.
3. Local nodes, or $\mathbf{u}$ nodes, are all nodes that do not fit the previous two types. These are located either on the inside of the subdomain meshes, or on $\mathbf{S}_\sigma$; e.g. nodes 1.11 and 3.2 in Figure 5.

For a problem with n_f displacement freedoms per node, these node types carry $2n_f$, $2n_f$ and n_f freedoms, respectively.

For nonmatching meshes it may be necessary to consider four node types if multiplier and displacement freedoms on partition boundaries do not coincide. The fourth type includes the so-called "multiplier nodes" or λ nodes, which are identified by a cross symbol.

5.1 Localized Multiplier System Equations

The component-by-component interpolations of subdomain quantities are

$$d_i^m = \mathbf{N}_{di}^m\,\mathbf{d}^m, \quad r_i^m = \mathbf{R}_i^m\,\boldsymbol{\alpha}^m, \quad \lambda_{\ell i}^m = \mathbf{N}_{\lambda i}^m\,\boldsymbol{\lambda}_\ell^m, \quad \bar{t}_i^m = \mathbf{N}_{ti}^m\,\bar{\mathbf{t}}^m, \quad \bar{f}_i^m = \mathbf{N}_{fi}^m\,\bar{\mathbf{f}}^m, \tag{35}$$

whereas displacement components of the partition frame are interpolated globally:

$$u_{bi} = \mathbf{N}_{bi}\,\mathbf{u}_b. \tag{36}$$

Grouping these components gives the complete field interpolations

$$\begin{aligned} \{d^m\} = \mathbf{N}_d^m\,\mathbf{d}^m, \quad \{r^m\} = \mathbf{R}^m\boldsymbol{\alpha}^m \quad \{\lambda_\ell^m\} = \mathbf{N}_\lambda^m\,\boldsymbol{\lambda}_\ell^m, \\ \{\bar{t}^m\} = \mathbf{N}_t^m\,\bar{\mathbf{t}}^m, \quad \{\bar{f}^m\} = \mathbf{N}_f^m\,\mathbf{f}^m, \quad \{u_b\} = \mathbf{N}_b\,\mathbf{u}_b. \end{aligned} \tag{37}$$

Here array $\mathbf{N}_d^m$ collects the shape functions for the deformational displacement in subdomain m, and similarly for the others. Node values are stacked in subdomain arrays $\mathbf{d}^m$, $\boldsymbol{\lambda}^m$, $\bar{\mathbf{t}}^m$ and $\bar{\mathbf{f}}^m$, and in the global array $\mathbf{u}_b$. For example, if Figure 5 represents a plane stress mesh, $\mathbf{d}^m$ and $\boldsymbol{\lambda}^m$ have dimension 38 and 16, respectively, for $m = 2$, whereas $\mathbf{u}_b$ has dimension 28. Prescribed displacements, if any, are included in the interpolation of $\{u_b\}$.

The interpolation for the subdomain rigid body displacements, $\{r^m\} = \mathbf{R}^m\boldsymbol{\alpha}^m$, is special in that $\boldsymbol{\alpha}^m$ are nodeless variables associated with a subdomain rather than a node. For example, if Figure 5 is a plane stress mesh, each subdomain has three RBMs, $\boldsymbol{\alpha}^m$ has dimension 3 and $\mathbf{R}^m$ is 2×3 for each $m = 1, 2, 3$. We shall assume that the deformational-RBM orthogonality condition (16) is also enforced over each discretized subdomain.

The strain interpolation can be expressed as $\{\epsilon^m\} = \mathbf{S}^m\,\mathbf{d}^m$, where the strain-displacement matrix $\mathbf{S}^m$ is constructed from the symmetric gradient of $\mathbf{N}_d^m$. The stress interpolation is $\{\sigma^m\} = \mathbf{E}^m\{\epsilon^m\}$, where $\mathbf{E}^m$ collects the constitutive moduli in matrix form.

Substituting these interpolations into Π_{PEM2} produces the discrete functional :

$$\hat{\Pi}_{\text{PEM2}}(\mathbf{d}, \boldsymbol{\alpha}, \boldsymbol{\lambda}_\ell, \mathbf{u}_b,) \; = \sum_m \Big[\, \hat{\Pi}^m_{\text{PEM2a}}(\mathbf{d}^m, \boldsymbol{\alpha}^m, \lambda^m_\ell) - \hat{\Pi}^m_{\text{PEM2b}}(\boldsymbol{\lambda}^m_\ell, \mathbf{u}_b)\Big] \tag{38}$$

The splitting (38) does not correspond to $\Pi^m_{\text{PE}} + \pi^m_u$, but simplifies the physical visualization of the discrete equations. Here

$$\hat{\Pi}^m_{\text{PEM2a}} = \begin{bmatrix} \mathbf{d}^m \\ \boldsymbol{\alpha}^m \\ \boldsymbol{\lambda}^m_\ell \end{bmatrix}^T \left\{ \frac{1}{2} \begin{bmatrix} \mathbf{K}^m_{dd} & \mathbf{0} & \mathbf{B}^m_{d\lambda} \\ \mathbf{0} & \mathbf{0} & \mathbf{R}^m_{\alpha\lambda} \\ \mathbf{B}^m_{\lambda d} & \mathbf{R}^m_{\lambda\alpha} & \mathbf{0} \end{bmatrix} \begin{bmatrix} \mathbf{d}^m \\ \boldsymbol{\alpha}^m \\ \boldsymbol{\lambda}^m_\ell \end{bmatrix} + \frac{1}{2} \begin{bmatrix} \mathbf{M}^m_{dd} & \mathbf{0} & \mathbf{0} \\ \mathbf{0} & \mathbf{M}^m_{\alpha\alpha} & \mathbf{0} \\ \mathbf{0} & \mathbf{0} & \mathbf{0} \end{bmatrix} \begin{bmatrix} \ddot{\mathbf{d}}^m \\ \ddot{\boldsymbol{\alpha}}^m \\ \ddot{\boldsymbol{\lambda}}^m_\ell \end{bmatrix} - \begin{bmatrix} \mathbf{f}^m_d \\ \mathbf{f}^m_\alpha \\ \mathbf{0} \end{bmatrix} \right\} \tag{39}$$

represents the contribution of the m^{th} subdomain plus the action of localized multipliers on its internal fields, whereas

$$\hat{\Pi}^m_{\text{PEM2b}} = \begin{bmatrix} \boldsymbol{\lambda}^m_\ell \\ \mathbf{u}^m_b \end{bmatrix}^T \begin{bmatrix} \mathbf{0} & \mathbf{C}^m_{\lambda u} \\ \mathbf{C}^m_{u\lambda} & \mathbf{0} \end{bmatrix} \begin{bmatrix} \boldsymbol{\lambda}^m \\ \mathbf{u}^m_b \end{bmatrix} = \begin{bmatrix} \boldsymbol{\lambda}^m_\ell \\ \mathbf{u}_b \end{bmatrix}^T \begin{bmatrix} \mathbf{0} & \mathbf{C}^m_{\lambda u}\mathbf{B}^m_b \\ (\mathbf{B}^m_b)^T\mathbf{C}^m_{u\lambda} & \mathbf{0} \end{bmatrix} \begin{bmatrix} \boldsymbol{\lambda}^m \\ \mathbf{u}_b \end{bmatrix}, \tag{40}$$

represents the contribution of the partition frame displacements. In (40), $\mathbf{u}^m_b = \mathbf{B}^m_b \mathbf{u}_b$ is the portion of $\mathbf{u}_b$ that contributes to subdomain m and $\mathbf{B}^m_b$ is the Boolean matrix that restricts $\mathbf{u}_b$ to $\mathbf{u}^m_b$.

The matrices and vectors appearing in (39)-(40) have the following expressions:

$$\begin{aligned}
\mathbf{K}^m_{dd} &= \int_{\Omega^m} (\mathbf{S}^m)^T\, \mathbf{E}^m\, \mathbf{S}^m\, d\Omega, \qquad & \mathbf{B}^m_{d\lambda} &= \int_{\partial\Omega^m_b} (\mathbf{N}^m_d)^T\, \mathbf{N}^m_\lambda\, d\Omega = (\mathbf{B}^m_{\lambda d})^T, \\
\mathbf{M}^m_{dd} &= \int_{\Omega^m} \rho^m\, (\mathbf{N}^m_d)^T \mathbf{N}^m_d\, d\Omega, \qquad & \mathbf{R}^m_{\alpha\lambda} &= \int_{\partial\Omega^m_b} (\mathbf{R}^m)^T\, \mathbf{N}^m_\lambda\, dS = (\mathbf{R}^m_{\lambda\alpha})^T, \\
\mathbf{M}^m_{\alpha\alpha} &= \int_{\Omega^m} \rho^m\, (\mathbf{R}^m)^T\, \mathbf{R}^m\, d\Omega, \qquad & \mathbf{C}^m_{u\lambda} &= \int_{\partial\Omega^m_b} \mathbf{N}^T_u\, \mathbf{N}^m_\lambda\, d\Omega = (\mathbf{C}^m_{\lambda u})^T, \\
\mathbf{f}^m_d &= \int_{\Omega^m} (\mathbf{N}^m_d)^T \mathbf{N}^m_f\, d\Omega\; \bar{\mathbf{f}}^m + \int_{\partial\Omega^m_\sigma} (\mathbf{N}^m_d)^T \mathbf{N}^m_t\, dS\; \bar{\mathbf{t}}^m, \\
\mathbf{f}^m_\alpha &= \int_{\Omega^m} (\mathbf{R}^m)^T \mathbf{N}^m_f\, d\Omega\; \bar{\mathbf{f}}^m + \int_{\partial\Omega^m_\sigma} (\mathbf{R}^m)^T \mathbf{N}^m_t\, dS\; \bar{\mathbf{t}}^m.
\end{aligned} \tag{41}$$

Setting $\delta\, \hat{\Pi}^m_{\text{PEM2}} = 0$ yields the discrete governing equations for each subdomain:

$$\begin{bmatrix} \mathbf{K}^m_{dd} & \mathbf{0} & \mathbf{B}^m_{d\lambda} & \mathbf{0} \\ \mathbf{0} & \mathbf{0} & \mathbf{R}^m_{\alpha\lambda} & \mathbf{0} \\ \mathbf{B}^m_{\lambda d} & \mathbf{R}^m_{\lambda\alpha} & \mathbf{0} & -\mathbf{C}^m_{\lambda u} \\ \mathbf{0} & \mathbf{0} & -\mathbf{C}^m_{u\lambda} & \mathbf{0} \end{bmatrix} \begin{bmatrix} \mathbf{d}^m \\ \boldsymbol{\alpha}^m \\ \boldsymbol{\lambda}^m_\ell \\ \mathbf{u}^m_b \end{bmatrix} + \begin{bmatrix} \mathbf{M}^m_{dd} & \mathbf{0} & \mathbf{0} & \mathbf{0} \\ \mathbf{0} & \mathbf{M}^m_{\alpha\alpha} & \mathbf{0} & \mathbf{0} \\ \mathbf{0} & \mathbf{0} & \mathbf{0} & \mathbf{0} \\ \mathbf{0} & \mathbf{0} & \mathbf{0} & \mathbf{0} \end{bmatrix} \begin{bmatrix} \ddot{\mathbf{d}}^m \\ \ddot{\boldsymbol{\alpha}}^m \\ \ddot{\boldsymbol{\lambda}}^m_\ell \\ \ddot{\mathbf{u}}^m_b \end{bmatrix} = \begin{bmatrix} \mathbf{f}^m_d \\ \mathbf{f}^m_\alpha \\ \mathbf{0} \\ \mathbf{0} \end{bmatrix} \tag{42}$$

The complete node value vectors $\mathbf{d}$, $\boldsymbol{\alpha}$, $\boldsymbol{\lambda}_\ell$ are obtained by stacking up the contributions of the N_s subdomains:

$$\mathbf{d} = \begin{bmatrix} \mathbf{d}^1 \\ \vdots \\ \mathbf{d}^{N_s} \end{bmatrix}, \quad \boldsymbol{\alpha} = \begin{bmatrix} \boldsymbol{\alpha}^1 \\ \vdots \\ \boldsymbol{\alpha}^{N_s} \end{bmatrix}, \quad \boldsymbol{\lambda}_\ell = \begin{bmatrix} \boldsymbol{\lambda}^1 \\ \vdots \\ \boldsymbol{\lambda}^{N_s} \end{bmatrix} \tag{43}$$

To establish the complete system equations in terms of the above relations, stack all subdomain matrices in block diagonal form, and link $\mathbf{u}_b^m = \mathbf{B}_b^m \mathbf{u}_b$:

$$\begin{bmatrix} \mathbf{K}_{dd} & \mathbf{0} & \mathbf{B}_{d\lambda} & \mathbf{0} \\ \mathbf{0} & \mathbf{0} & \mathbf{R}_{\alpha\lambda} & \mathbf{0} \\ \mathbf{B}_{\lambda d} & \mathbf{R}_{\lambda\alpha} & \mathbf{0} & -\mathbf{C}_{\lambda u} \\ \mathbf{0} & \mathbf{0} & -\mathbf{C}_{u\lambda} & \mathbf{0} \end{bmatrix} \begin{bmatrix} \mathbf{d} \\ \boldsymbol{\alpha} \\ \boldsymbol{\lambda}_\ell \\ \mathbf{u}_b \end{bmatrix} + \begin{bmatrix} \mathbf{M}_{dd} & \mathbf{0} & \mathbf{0} & \mathbf{0} \\ \mathbf{0} & \mathbf{M}_{\alpha\alpha} & \mathbf{0} & \mathbf{0} \\ \mathbf{0} & \mathbf{0} & \mathbf{0} & \mathbf{0} \\ \mathbf{0} & \mathbf{0} & \mathbf{0} & \mathbf{0} \end{bmatrix} \begin{bmatrix} \ddot{\mathbf{d}} \\ \ddot{\boldsymbol{\alpha}} \\ \ddot{\boldsymbol{\lambda}}_\ell \\ \ddot{\mathbf{u}}_b \end{bmatrix} = \begin{bmatrix} \mathbf{f}_d \\ \mathbf{f}_\alpha \\ \mathbf{0} \\ \mathbf{0} \end{bmatrix}, \tag{44}$$

where $\mathbf{C}_{\lambda u} = \sum_m \mathbf{C}_{\lambda u}^m \mathbf{B}_b^m = \mathbf{C}_{u\lambda}^T$. In the static case the term involving accelerations drops out.

5.2 Forming Stiffness and Mass from Existing FEM Libraries

The foregoing matrix equations involve $\mathbf{K}_{dd}^m$, $\mathbf{M}_{dd}^m$ and $\mathbf{M}_{\alpha\alpha}^m$. These are the deformation-basis stiffness, deformation-basis mass and rigid-body motion mass matrices, respectively, for an individual subdomain. In practice these can be obtained from a standard finite element library as follows:

1. Using the available library, form the stiffness matrix $\mathbf{K}^m$ and mass matrix $\mathbf{M}^m$ for the subdomain m by standard assembly techniques.
2. Extract a rigid-body mode basis $\boldsymbol{\Phi}_\alpha^m$ and a deformational basis $\boldsymbol{\Phi}_d^m$ from the null and range space, respectively, of $\mathbf{K}^m$.
3 Orthonormalize so that $\boldsymbol{\Phi}_d^m$ and $\boldsymbol{\Phi}_\alpha^m$ are biorthogonal with respect to $\mathbf{M}^m$. Take $\mathbf{R}^m = \boldsymbol{\Phi}_\alpha^m$.
4. Set $\mathbf{K}_{dd}^m = (\boldsymbol{\Phi}_d^m)^T \mathbf{K}^m \boldsymbol{\Phi}_d^m$, $\mathbf{M}_{dd}^m = (\boldsymbol{\Phi}_d^m)^T \mathbf{M}^m \boldsymbol{\Phi}_d^m$, $\mathbf{M}_{\alpha\alpha}^m = (\mathbf{R}^m)^T \mathbf{M}^m \mathbf{R}^m$.

For the static case one simply takes $\mathbf{K}_{dd}^m = \mathbf{K}^m$, making maximum use of existing FEM libraries. It is necessary to extract the rigid body basis $\mathbf{R}^m$, although this is not required to satisfy the mass orthogonality condition. In the dynamic case the procedure is more delicate; there is no explicit need, however, to explicitly compute the deformation modes $\boldsymbol{\Phi}_d^m$ as shown by Park, Gumaste and Alvin.[32]

5.3 Specializations

Equations (44) are valid for matching as well as nonmatching meshes. For matched meshes with node-force-collocated multipliers, $\mathbf{B}_{d\lambda}$, $\mathbf{R}_{\alpha\lambda}$ and $\mathbf{C}_{u\lambda}$ reduce to $\mathbf{B}_b$, $\mathbf{R}_b = \mathbf{B}_b^T \mathbf{R}$ and $\mathbf{C}_b = \mathbf{B}_b^T \mathbf{L}$, respectively. Here $\mathbf{B}_b^T$ is a Boolean localization matrix that localizes the interface degrees of freedom, and $\mathbf{L}$ is the global assembly matrix such that $\mathbf{K}_g = \mathbf{L}^T \mathbf{K} \mathbf{L}$ is the global stiffness matrix of the non-partitioned structure. This is the equation used in the development of a simple dynamic parallel algorithm.[32]

For static problems the inertial terms are dropped and $\mathbf{K}_{dd}$ may be kept as $\mathbf{K}$ (the block diagonal supermatrix of all $\mathbf{K}^m$), giving

$$\begin{bmatrix} \mathbf{K} & \mathbf{0} & \mathbf{B}_b & \mathbf{0} \\ \mathbf{0} & \mathbf{0} & \mathbf{R}_b^T & \mathbf{0} \\ \mathbf{B}_b^T & \mathbf{R}_b & \mathbf{0} & -\mathbf{C}_b \\ \mathbf{0} & \mathbf{0} & -\mathbf{C}_b^T & \mathbf{0} \end{bmatrix} \begin{bmatrix} \mathbf{d} \\ \boldsymbol{\alpha} \\ \boldsymbol{\lambda}_\ell \\ \mathbf{u}_b \end{bmatrix} = \begin{bmatrix} \mathbf{f}_d \\ \mathbf{f}_\alpha \\ \mathbf{0} \\ \mathbf{0} \end{bmatrix} \tag{45}$$

The nodal deformation vector $\mathbf{d}$ can be obtained from the first matrix equation as $\mathbf{d} = \mathbf{F}(\mathbf{f}_d - \mathbf{B}_b \boldsymbol{\lambda}_\ell)$, where $\mathbf{F} = \mathbf{K}^+$ is the free-free flexibility, or Moore-Penrose generalized inverse of $\mathbf{K}$. This matrix can be efficiently obtained, subdomain by subdomain, as described in Felippa, Park and Justino.[34] Substituting this into the third row gives $\mathbf{B}_b^T \mathbf{F} \mathbf{B}_b \boldsymbol{\lambda}_\ell - \mathbf{R}_b \boldsymbol{\alpha} + \mathbf{C}_b \mathbf{u}_b = \mathbf{B}_b^T \mathbf{F} \mathbf{f}_d$. Combining the second and fourth

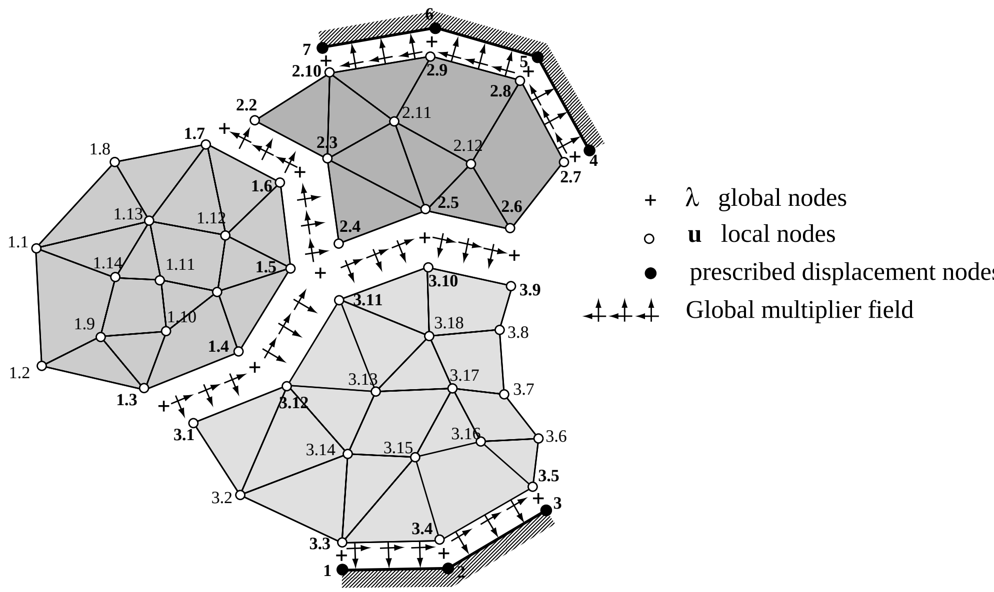

Figure 6. Matching-mesh, global-multiplier FEM discretization of example domain of Figure 1(c). Three node types are identified by indicated symbols. Prescribed displacement portions of the boundary are treated as internal interfaces.

rows with that equation, one arrives at the following partitioned flexibility equation:

$$\begin{bmatrix} \mathbf{F}_b & -\mathbf{R}_b & -\mathbf{C}_b \\ -\mathbf{R}_b^T & \mathbf{0} & \mathbf{0} \\ -\mathbf{C}_b^T & \mathbf{0} & \mathbf{0} \end{bmatrix} \begin{bmatrix} \boldsymbol{\lambda}_\ell \\ \boldsymbol{\alpha} \\ \mathbf{u}_b \end{bmatrix} = \begin{bmatrix} \mathbf{h}_b \\ \mathbf{f}_\alpha \\ \mathbf{0} \end{bmatrix} \tag{46}$$

where $\mathbf{F}_b = \mathbf{B}_b^T\,\mathbf{F}\,\mathbf{B}_b$ and $\mathbf{h}_b = \mathbf{B}_b^T\,\mathbf{F}\,\mathbf{f}_d$. The latter has dimensions of displacement. Equation (46) links only the interface degrees of freedom.

The partitioned flexibility equation (46) and its dynamic counterpart have been applied to parallel computations by Park, Justino and Felippa,[35,36] treatment of hetrogeneities,[33] to damage detection by Park, Reich and Alvin,[37] to joint identification by Park and Felippa,[38] and to distributed vibration control problems by Park and Kim.[39]

5.4 Global Multiplier FEM Discretization

Figure 6 shows a matched-mesh, FEM discretization of the example domain using global multipliers. The governing equations can be derived, for example, from the Π_{PEM1} functional. The details will not be worked out here, as they essentially lead to the equations summarized in Section 6.4.

It should be remarked that nodes with prescribed displacements can be treated in two ways. The one shown in Figure 6 carries additional multiplier and displacement unknowns, It leads, however, to a more modular implementation of the floating subdomain problem since all subdomains can be treated as free-free, while support boundary conditions are applied by the interface solver. In addition, the multipliers give directly the reactions, which are often of interest. Alternatively, the displacement conditions could be applied directly on the subdomain nodes, and the multipliers on $\partial\Omega_u$ dispensed with.

6. RELATED PRIOR WORK

This section summarizes specific publications or lines of research that have directly or indirectly influenced the work presented here. The notational scheme used by other authors has been modified as necessary to agree with our nomenclature.

6.1 The Classical Force Method

Suppose the subdomains depicted in Figure 6 are an assembly of substructures connected by force-collocated global Lagrange multipliers arrayed in $\boldsymbol{\lambda}_b$. These are taken as the redundant forces of the Classical Force Method. The governing matrix equations for this method[1,40] may be compactly presented in the supermatrix form

$$\begin{bmatrix} \mathbf{F} & -\mathbf{I} & \mathbf{0} \\ -\mathbf{I} & \mathbf{0} & \mathbf{B}_1 \\ \mathbf{0} & \mathbf{B}_1^T & \mathbf{0} \end{bmatrix} \begin{bmatrix} \mathbf{p} \\ \mathbf{v} \\ \boldsymbol{\lambda}_b \end{bmatrix} = \begin{bmatrix} \mathbf{0} \\ -\mathbf{B}_0\,\mathbf{f}_b \\ \mathbf{0} \end{bmatrix}. \tag{47}$$

Once this equation is solved, the interface displacement $\mathbf{u}_b$ can be recovered from

$$\mathbf{u}_b = \mathbf{B}_0^T\,\mathbf{v} = \mathbf{F}_b\,\mathbf{f}_b, \tag{48}$$

in which $\mathbf{F}_b = \mathbf{D}_{00} - \mathbf{D}_{10}^T\mathbf{D}_{11}^{-1}\mathbf{D}_{10} = \mathbf{K}_b^{-1}$, $\mathbf{D}_{11} = \mathbf{B}_1^T\,\mathbf{F}\,\mathbf{B}_1$ and $\mathbf{D}_{10} = \mathbf{B}_1^T\,\mathbf{F}\,\mathbf{B}_0$.

In these equations $\mathbf{f}_b$, $\mathbf{p}$ and $\boldsymbol{\lambda}_b$ are vectors of applied, internal and redundant forces, respectively; $\mathbf{u}_b$ and $\mathbf{v}$ are the vectors of node displacements and internal deformations work-conjugate to $\mathbf{f}_b$ and $\mathbf{p}$, respectively; $\mathbf{B}_0$ and $\mathbf{B}_1$ are matrices that decompose the internal forces into statically determinate and indeterminate components, respectively; finally, $\mathbf{F}$ denotes the block-diagonal deformational flexibility matrix $\mathbf{diag}\{\mathbf{F}^m\}$, in which $\mathbf{F}^m$ is the deformational-flexibility matrix of the m^{th} substructure. Both the deformation flexibility $\mathbf{F}$ and the so-called indeterminate flexibility $\mathbf{D}_{11}$ are required to be non-singular. If the structure is statically determinate, $\mathbf{B}_1$ and $\boldsymbol{\lambda}_b$ are void, and internal forces $\mathbf{p}$ can be determined directly from statics.

The challenge for implementing this method is the effective selection of the indeterminate force transmission matrix $\mathbf{B}_1$. Once this is done, $\mathbf{B}_0$ can be easily formed and all other quantities thereby obtained. Hence, most papers on the Classical Force Method have focused on the algorithmic construction of $\mathbf{B}_1$ through clever choices of redundant force patterns. See, for instance, the surveys by Kaveh[41] and Felippa.[42,43] Because $\mathbf{D}_{11}$ is full or quite dense, however, this method has not been competitive against the Direct Stiffness Method version of the displacement method, particularly for the continuum FEM models that became popular in the 1960s. These points are further elaborated by Felippa and Park.[44]

Comparing the Classical Force Method (47) and (48) with the partitioned flexibility equations (45) and (46), we find that nothing in the latter requires user decisions or elaborated analysis of redundants. Once the meshes and partitions are set up, and rigid body mode bases obtained, matrices $\mathbf{B}$, $\mathbf{R}_b$ and $\mathbf{C}_b$ follow, and hence the construction of the partitioned flexibility equation (45) is automatic. The efficient solution of (45) is discussed by Park, Justino and Felippa[35,36] and that of its dynamic counterpart by Park, Gumaste and Alvin.[32]

In passing, we mention that Professor Gallagher had been pursuing the development of a 'modernized' force method for structural shape and topology optimization.[45] At this writing, the potential of the present partitioned flexibility equations (45) or its variants for use in such applications remains unexplored.

6.2 Fraeijs de Veubeke (1973)

A particularly relevant work is that presented by Fraeijs de Veubeke in a workshop lecture on Matrix Structural Analysis delivered at the University of Calgary in 1973.[22] The material examines in great detail intrinsic and connection properties of a discretized structure divided into arbitrary elements, with no *a priori* preconceptions on element types. He spelled out the following matrix relations (italics below denote Fraeijs de Veubeke's terminology):

a) *Transition conditions* between face $+$ and face $-$ of each interface:

$$\begin{aligned} \text{Displacements:} \quad & \mathbf{u}^{+} - \mathbf{u}^{-} = \mathbf{0} \\ \text{Tractions:} \quad & \mathbf{t}^{+} + \mathbf{t}^{-} \ \ = \mathbf{0} \end{aligned} \tag{49}$$

b) *Statics at element level*:

$$\mathbf{R}^{T}(\mathbf{f} + \mathbf{f}_b) = \mathbf{0}, \tag{50}$$

where (in our notation) $\mathbf{R}$ is a basis for the element rigid body modes, and $\mathbf{f}_b$ and $\mathbf{f}$ are force vectors produced by boundary loads and body forces, respectively.

c) *Generalized boundary displacement vector*:

$$\mathbf{u}_b = \mathbf{F}\,(\mathbf{f} + \mathbf{f}_b) + \mathbf{R}\,\boldsymbol{\alpha}, \tag{51}$$

where $\mathbf{F}$ is the deformational flexibility matrix and $\boldsymbol{\alpha}$ are rigid body amplitudes.

These key relations, also summarized in Table 1, provide the necessary tools to extend flexibility-based methods beyond the Classical Force Method, which by then had already hit a dead end.[43] Unfortunately the lecture did not provide the all-important implementation details. Furthermore the Notes were of limited dissemination, having only appeared in the 1980 Memorial Volume of selected papers.

6.3 Atluri (1975)

In the previously cited 1975 paper, Atluri[6] presented a systematic construction of hybrid elasticity functionals for finite element development work. The approach is to combine

$$\text{Hybrid functional} \ = \ \text{Canonical internal functional} + \text{Interface potential} \tag{52}$$

From the canonical functionals of linear elasticity, Atluri selected the Hu-Washizu, Hellinger-Reissner, Potential Energy (Displacement) and Complementary Energy (Equilibrium) forms. Two interface potential forms, herein called π_u and π_λ, were considered. Of the various combinations studied by Atluri, those identified as HWM2 and HD2 are particularly relevant to the formulation of Section 3.

6.4 Farhat and Roux (1991, 1994)

The work of Farhat and Roux[23,24] develops a practical implementation of flexibility methods driven by a specific objective: the efficient solution of FEM structural equations on massively parallel computers. Their derivations are summarized in Table 1. The starting point is the constrained FEM stiffness equilibrium equations for a structure divided into matched subdomains:

$$\begin{bmatrix} \mathbf{K} & \mathbf{C}_\lambda \\ \mathbf{C}_\lambda^T & 0 \end{bmatrix} \begin{bmatrix} \mathbf{u} \\ \boldsymbol{\lambda}_b \end{bmatrix} = \begin{bmatrix} \mathbf{f} \\ \mathbf{0} \end{bmatrix} \tag{53}$$

Table 1 Comparisons of De Veubeke, Atluri, Farhat/Roux, and Present Formulations

	De Veubeke (1973)	Atluri (1975)	Farhat & Roux (1994)	Present and Park and Felippa[38]
Formulation Basis	Matrix methods of structural analysis	Continuum variational formulation	Equilibrium with constraints	Continuum variational formulation
Lagrangian multiplier	Global and generalized forces	Local and weighted average forces	Global and generalized forces	Local and physical point forces
Flexibility Matrix	$\mathbf{F}$ (no detail)	not derived	$\mathbf{F} = \mathbf{C}_\lambda^T\ \mathbf{K}^+\ \mathbf{C}_\lambda$	$\mathbf{F}_b = \mathbf{B}_b^T\ \mathbf{K}^+\ \mathbf{B}_b$
Floating partition equilibrium	$\mathbf{R}^T(\mathbf{f} + \mathbf{f}_b) = \mathbf{0}$	not considered	$\mathbf{R}^T\ (\mathbf{f} + \mathbf{C}_\lambda\ \boldsymbol{\lambda}_b) = \mathbf{0}$	$\mathbf{R}^T\ \mathbf{B}_b\boldsymbol{\lambda}_\ell + \mathbf{f}_\alpha = \mathbf{0}$
Interface constraints	$\mathbf{u}^+ - \mathbf{u}^- = \mathbf{0}$	$\mathbf{B}_b\ \mathbf{u}$ $-\mathbf{C}_b\ \mathbf{u}_b = \mathbf{0}$	$\mathbf{C}_\lambda^T\ \mathbf{u} = \mathbf{0}$	$\mathbf{B}_b^T\ \mathbf{d} + \mathbf{R}_b\boldsymbol{\alpha}$ $-\mathbf{C}_b\ \mathbf{u}_b = \mathbf{0}$
Newton's 3rd law	$\mathbf{t}^+ + \mathbf{t}^- = 0$	$\mathbf{C}_{u\lambda}\ \boldsymbol{\lambda}_\ell = \mathbf{0}$	implicit in interface treatment	$\mathbf{C}_b^T\ \boldsymbol{\lambda}_\ell = \mathbf{0}$

Here $\mathbf{K}$ is the partitioned block-diagonal partitioned stiffness matrix, $\mathbf{C}_\lambda$ the constraint matrix that enforces the interdomain continuity condition $\mathbf{u}^+ = \mathbf{u}^-$, $\mathbf{u}$ is the interior node displacement vector, $\mathbf{f}$ the applied node force vector, and $\boldsymbol{\lambda}_b$ is the vector of node-force-collocated Lagrange multipliers. Solving for $\mathbf{u}$ from the first row of (53) one gets

$$\mathbf{u} = \mathbf{K}^+(\mathbf{f} - \mathbf{C}_\lambda\ \boldsymbol{\lambda}_b) + \mathbf{R}\ \boldsymbol{\alpha}. \tag{54}$$

Here $\mathbf{K}^+$ is a generalized inverse of $\mathbf{K}$, $\mathbf{R}$ is a null-space basis of $\mathbf{K}$ whenever $\mathbf{K}$ is rank-deficient because of unsuppressed rigid body modes, and $\boldsymbol{\alpha}$ collects those modal amplitudes. Substituting (54) into the second row of (53) yields

$$\mathbf{C}_\lambda^T\ [\mathbf{K}^+\ (\mathbf{f} - \mathbf{C}_\lambda\ \boldsymbol{\lambda}_b) + \mathbf{R}\ \boldsymbol{\alpha}\ ] = \mathbf{0}. \tag{55}$$

Grouping (55) with the self-equilibrium equation (50) applied at the subdomain level, in which $\mathbf{f}_b = -\mathbf{C}_\lambda\boldsymbol{\lambda}_b$, one arrives at

$$\begin{bmatrix} \mathbf{C}_\lambda^T\ \mathbf{K}^+\ \mathbf{C}_\lambda & -\mathbf{C}_\lambda^T\ \mathbf{R} \\ -\mathbf{R}^T\ \mathbf{C}_\lambda & \mathbf{0} \end{bmatrix} \begin{bmatrix} \boldsymbol{\lambda}_b \\ \boldsymbol{\alpha} \end{bmatrix} = \begin{bmatrix} \mathbf{C}_\lambda^T\ \mathbf{K}^+\ \mathbf{f} \\ -\mathbf{R}^T\ \mathbf{f} \end{bmatrix}. \tag{56}$$

which contains only interface variables. Equation (56) is solved iteratively by projected conjugate-gradient methods. Upon convergence the interior subdomain states are recovered from (54). Farhat and coworkers have developed projection operators that offer parallel scalability for structural problems, not only for three-dimensional solid elasticity problems but for plates and shells as well.[25,26] These parallel structural algorithms, collectively identified as FETI (Finite Element Tearing and Interconnecting), represent one of the major advances in computational structural mechanics over the past decade.

6.5 Interface Potentials Accounting for Jump Conditions

In a recent survey of Parametrized Variational Principles, one of the authors presented[46] a two-parameter, four-field form interface potential form that can be reduced to specific instances by adjusting the parameters. The varied local fields are the interface displacements u_i and the boundary tractions $\sigma_{ni} = \sigma_{ij} n_j$ coming from the FEM mesh. The varied interface fields are the tractions t_i and the partition frame displacements u_{bi}. The two faces are labeled $-$ and $+$. A generalization over the potentials considered previously is the allowance of displacement and traction jumps at any point of the interface:

$$[\![u_i]\!] = u_i^+ - u_i^-, \qquad [\![t_i]\!] = \sigma_{ni}^+ + \sigma_{ni}^- \qquad \text{on} \quad \partial\Omega_b. \tag{57}$$

If the "transition conditions" (49) are verified both jumps vanish. Prescribed jumps are resolved by setting

$$u_i^+ = u_{bi} + \tfrac{1}{2}[\![u_i]\!], \quad u_i^- = u_{bi} - \tfrac{1}{2}[\![u_i]\!], \quad \sigma_{ni}^+ = t_i + \tfrac{1}{2}[\![t_i]\!], \quad \sigma_{ni}^- = -t_i + \tfrac{1}{2}[\![t_i]\!], \tag{58}$$

where $u_{bi} = (u_i^+ + u_i^-)/2$ and $t_i = (\sigma_{ni}^+ - \sigma_{ni}^-)/2$. The parametrized interface functional that treats all of the above as weak constraints is

$$\begin{aligned}\pi(u_i, \sigma_{ni}, u_{bi}, t_i) = \int_{\partial\Omega_b} \Big[&\big(2(\alpha_1 - \alpha_2)\, t_i + \alpha_2(\sigma_{ni}^+ - \sigma_{ni}^-)\big)\,(u_i^+ - u_i^- - [\![u_i]\!]) + \alpha_1 [\![t_i]\!](u_i^+ + u_i^-) \\ &+ (1 - 2\alpha_1)\,\big(\sigma_{ni}^+(u_i^+ - u_{bi} - \tfrac{1}{2}[\![u_i]\!]) + \sigma_{ni}^-(u_i^- - u_{bi} + \tfrac{1}{2}[\![u_i]\!]) + u_{bi}\,[\![t_i]\!]\big)\Big]\, dS.\end{aligned} \tag{59}$$

Here α_1 and α_2 are free parameters. This generalizes a form proposed by Fraeijs de Veubeke in 1974.[15] The special case in which $\alpha_1 = \frac{1}{2}$, $\alpha_2 = 0$, $[\![u_i]\!] = 0$ and $[\![t_i]\!] = 0$ results in

$$\pi(u_i, t_i) = \int_{\partial\Omega_b} t_i\,(u_i^+ - u_i^-)\, dS, \tag{60}$$

which with the notational change $t_i \to \lambda_{bi}$ becomes the π_λ of the method of global Lagrange multipliers introduced in Section 3.5. Setting $\alpha_1 = \alpha_2 = 0$ together with $[\![u_i]\!] = 0$ and $[\![t_i]\!] = 0$ results in

$$\pi(u_i, \sigma_{ni}, u_{bi}) = \int_{\partial\Omega_b} \big[\sigma_{ni}^+(u_i^+ - u_{bi}) + \sigma_{ni}^-\,(u_i^- - u_{bi})\big]\, dS, \tag{61}$$

which with the notational change $\sigma_{ni}^+ \to \lambda_{\ell i}^+$ and $\sigma_{ni}^- \to \lambda_{\ell i}^-$ becomes the π_u of the method of localized Lagrange multipliers introduced in Section 3.2.

While an actual displacement jump is uncommon (aside from contact, impact and crack propagation problems), traction jumps can occur on physical interfaces, such as joints, subject to interface loads or wave propagation. This extension of partitioned analysis is under investigation.

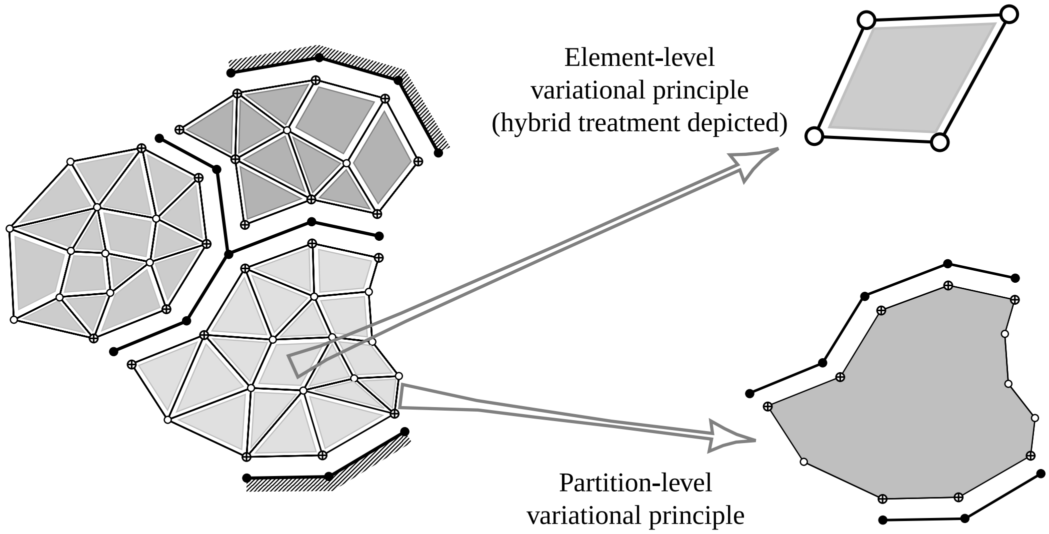

Figure 7. Multilevel/hierarchical use of variational principles. The variational principle(s) used for development of individual elements may be different from that used for partitions that groups such elements. This strategy is generally inevitable if a partition contain different element types.

7. SUMMARY AND CONCLUSIONS

We have presented a continuum-based variational formulation for the partitioned analysis of linear structural systems. The varied fields are the deformational and rigid body displacements of each partition, the global displacements of partition frames, and localized Lagrange multipliers that enforce interface displacement compatibility.

The most important ingredients of the variational formulation are: the use of localized Lagrange multiplier fields, and the decomposition of the substructural displacements into deformational and rigid-body. The latter is instrumental in providing separate equilibrium equations for each partition viewed as a rigid body and as a flexible body. This separation is important in implementing accurate dynamic time-stepping solvers as well as handling floating subdomains. The multiplier localization simplifies the treatment of non-matching mesh interfaces, as well as that of cross points in matched interfaces.

The discrete equations were obtained using the Potential Energy canonical functional for the internal fields. This was done for expediency since the paper focuses on the treatment of the interfaces. Nothing prohibits the use of internal functionals with independently varied stress and/or strain fields, such as the Hu-Washizu or Hellinger-Reissner principles or, more generally, parametrized variational forms.[11,46]

In practice, however, the application of variational principles to partitioned analysis is best viewed in a *multilevel/hierarchical* framework. This is illustrated in Figure 7. The variational principle(s) used to develop individual elements need not be the same as that used to link up the partitions, as long as they produce elements with the standard displacement degrees of freedom. In fact the key ingredient for the partition-level principle is the interface potential rather than the interior functional. Two advantages of this approach should be noted:

a) If partitions combine distinct elements types, it is likely that they come from different variational formulations. Hence a multilevel strategy is inevitable.

b) It simplifies the use of element matrices from existing FEM libraries. In the case of models assembled from commercial software, the element formulation basis is often unknown. Coupling techniques that do not require such information are obviously preferable from the standpoint of modularity. As noted in the Introduction, partitioned analysis should ideally focus on modeling the interaction separately from the components.

The question of how to select interface interpolation functions to maintain rank sufficiency and consistency (the latter being verifiable by interface patch tests) remains a topic of current research.

Two related topics are addressed in separate papers. If the deformational displacement field is transformed into strains, the resulting equations have been found attractive for system identification, damage detection and localized vibration control, which collectively form a set of important inverse problems. These topics have been covered by Park, Reich and Alvin,[37] Park and Kim[39] and Park and Reich[47,48]. An extension of the present variational principle to interaction of flexible structures with an internal acoustic fluid has been developed by Park, Felippa and Ohayon.[49]. Recently, the partitioned formulation has been applied to substructuring technique[50] and reduced-order modeling[51].

Acknowledgments

The present work has been supported by the National Science Foundation under the grant High Performance Computer Simulation of Multiphysics Problems (award ECS-9725504) and by Sandia National Laboratories under the Accelerated Strategic Computational Initiative (ASCI) contracts AS-5666 and AS-9991.

References

1. J. H. Argyris and S. Kelsey, *Energy Theorems and Structural Analysis*, Butterworths, London (1960); reprinted from *Aircraft Engrg.* **26**, Oct-Nov 1954 and **27**, April-May 1955.

2. B. M. Fraeijs de Veubeke, 'Displacement and equilibrium models,' in *Stress Analysis*, ed. by O. C. Zienkiewicz and G. Hollister, Wiley, London, pp. 145–197, 1965.

3. K. Washizu, *Variational Methods in Elasticity and Plasticity*, Pergamon Press, New York, 1968.

4. T. H. H. Pian and P. Tong, 'Basis of finite element methods for solid continua,' *Int. J. Numer. Meth. Engrg.*, **1**, 3–29, 1969.

5. T. H. H. Pian, 'Finite element methods by variational principles with relaxed continuity requirements,' in *Variational Methods in Engineering*, Vol. 1, ed. by C. A. Brebbia and H. Tottenham, Southampton University Press, Southhampton, U.K., 1973.

6. S. N. Atluri, 'On "hybrid" finite-element models in solid mechanics,' In: *Advances in Computer Methods for Partial Differential Equations*. Ed. by R. Vichnevetsky, AICA, Rutgers University, 346–356, 1975.

7. J. T. Oden and J. N. Reddy, *Variational Methods in Theoretical Mechanics*, Springer-Verlag, 1982.

8. J. N. Reddy, *Energy and Variational Methods in Applied Mechanics*, Wiley/Interscience, New York, 1984.

9. T. J. R. Hughes, *The Finite Element Method: Linear Static and Dynamic Finite Element Analysis*, Prentice-Hall, Englewood Cliffs, N. J., 1987.

10. O. C. Zienkiewicz and R. E. Taylor, *The Finite Element Method*, Vol I, 4th ed. New York: McGraw-Hill, 1989.

11. C. A. Felippa, 'A survey of parameterized variational principles and applications to computational mechanics,' *Comp. Meth. Appl. Mech. Engrg.*, **113**, 109–139, 1994.

12. T. H. H. Pian, 'Derivation of element stiffness matrices by assumed stress distributions,' *AIAA J.*, **2**, 1333–1336, 1964.

13. L. R. Herrmann, ‘A bending analysis for plates,’ in *Proceedings 1st Conference on Matrix Methods in Structural Mechanics*, AFFDL-TR-66-80, Air Force Institute of Technology, Dayton, Ohio, pp. 577-604, 1966.

14. B. M. Fraeijs de Veubeke, ‘A new variational principle for finite elastic displacements,’ in *Int. J. Engng. Sci*, **10**, 745–763, 1972.

15. B. M. Fraeijs de Veubeke, 1974, ‘Variational principles and the patch test.’ *Int. J. Numer. Meth. Engrg.*, **8**, 783–801

16. R. Courant and D. Hilbert, *Methods of Mathematical Physics*, Vol I, Interscience, New York, 1953.

17. M. J. Sewell, *Maximum and Minimum Principles*. Cambridge, England, 1987.

18. J.-L. Lagrange, *Mécanique Analytique*, 1788, 1965 Edition complète, 2 vols., Blanchard, Paris, 1965.

19. C. Lanczos, *The Variational Principles of Mechanics*, Dover, New York, 4th ed., 1970.

20. R. Dugas, *A History of Mechanics*, Dover, New York, 332-338, 1988.

21. K. C. Park and C. A. Felippa, ‘A Variational Framework for Solution Method Developments in Structural Mechanics,’ *J. Appl. Mech.*, March 1998, **Vol. 65/1**, 242-249, 1998.

22. B. M. Fraeijs de Veubeke, ‘Matrix structural analysis: Lecture Notes for the International Research Seminar on the Theory and Application of Finite Element Methods,’ Calgary, Alberta, Canada, July-August 1973; reprinted in *B. M. Fraeijs de Veubeke Memorial Volume of Selected Papers*, ed. by M. Geradin, Sitthoff & Noordhoff, Alphen aan den Rijn, The Netherlands, 509–568, 1980.

23. C. Farhat and F.-X. Roux, ‘A method of finite element tearing and interconnecting and its parallel solution algorithm,’ *Int. J. Numer. Meth. Engrg.*, **32**, 1205-1227, 1991.

24. C. Farhat and F.-X. Roux, ‘Implicit parallel processing in structural mechanics,’ *Computational Mechanics Advances*, **2**, 1-124, 1994.

25. C. Farhat and J. Mandel, ‘The two-level FETI method for static and dynamic plate problems - Part I: an optimal iterative solver for biharmonic systems,’ *Comp. Meth. Appl. Mech. Engrg.*, 155, 129-151, 1998.

26. C. Farhat, P.-S. Chen, J. Mandel and F.-X. Roux, ‘The two-level FETI method for static and dynamic plate problems - Part II: Extension to shell problems, parallel implementation and performance results,’ *Comp. Meth. Appl. Mech. Engrg.*, 155, 153-179, 1998.

27. W. Prager, ‘Variational principles for linear elastostatics for discontinous displacements, strains and stresses,’ in *Recent Progress in Applied Mechanics*, The Folke-Odgvist Volume, ed. by B. Broger, J. Hult and F. Niordson, Almqusit and Wiksell, Stockholm, 463–474, 1967.

28. P. Tong, ‘New displacement finite element method for solid continua,’, *Int. J. Numer. Meth. Engrg.*, **2**, 73–83, 1970.

29. P. G. Bergan and M. K. Nygård, ‘Finite elements with increased freedom in choosing shape functions,’ *Int. J. Numer. Meth. Engrg.*, **20**, 643–664, 1984.

30. C. A. Felippa, ‘Parametrized multifield variational principles in elasticity: II. Hybrid functionals and the Free Formulation,’ *Commun. Appl. Numer. Meths*, **5**, 89–98, 1989

31. C. Bernardi, Y. Maday and A. T. Patera, ‘A new nonconforming appraoch to domain decomposition: the mortar element method,’ Technical Report, Université Pierre at Marie Curie, Paris, France, Jan 1990.

32. Gumaste, Udayan, Park, K. C. and Alvin, K. F. , “A Family of Implicit Partitioned Time Integration Algorithms for Parallel Analysis of Heterogeneous Structural Systems,” *Computational Mechanics: an International Journal*, **24** (2000) 6, 463-475.

33. Park, K. C., Gumaste, Udayan, and Felippa, C. A., “A Localized Version of the Method of Lagrange Multipliers and its Applications,” *Computational Mechanics: an International Journal*, **24** (2000) 6, 476-490.

34. C. A. Felippa, K. C. Park and M. R. Justino F., 'The construction of free-free flexibility matrices as generalized stiffness inverses,' *Computers & Structures*, **68**, 411-418, 1998.

35. M. R. Justino F., K. C. Park and C. A. Felippa, 'An algebraically partitioned FETI method for parallel structural analysis: implementation and numerical performance evaluation,' *Int. J. Numer. Meth. Engrg.*, **40**, 2739-2758, 1997.

36. K. C. Park, M. R. Justino F. and C. A. Felippa, 'An algebraically partitioned FETI method for parallel structural analysis: algorithm description,' *Int. J. Numer. Meth. Engrg.*, **40**, 2717-2737 (1997).

37. K. C. Park, G. W. Reich, and K. F. Alvin, 'Damage detection using localized flexibilities,' in : *Structural Health Monitoring, Current Status and Perspectives*, ed. by F.-K. Chang, Technomic Pub., 125–139, 1997.

38. K. C. Park and C. A. Felippa, 'A flexibility-based inverse algorithm for identification of structural joint properties,' Proc. *ASME Symposium on Computational Methods on Inverse Problems*, Anaheim, CA, 15-20 Nov 1998.

39. K. C. Park and N.-I. Kim, 'A Theory of Localized Vibration Control via Partitioned LQR Synthesis,' Center for Aerospace Structures, Report No. CU-CAS-98-13, University of Colorado, Boulder, CO, July 1998; also *Proceedings XXI Congresso Nacional de Matematica Applicada e Computacional*, Caxambu, MG, Brazil, Sep 1998.

40. E. C. Pestel and F. A. Leckie, *Matrix Methods in Elastomechanics*, McGraw-Hill, New York, 1963.

41. A. Kaveh, 'Recent developments in the force method of structural analysis,' *Applied Mech. Rev.*, **45(9)**, 401-418, 1992.

42. C. A. Felippa, 'Will the Force Method come back?,' *J. Appl. Mech.*, **54**, pp. 728–729, 1987.

43. C. A. Felippa, 'Parametric unification of matrix structural analysis: classical formulation and d-Connected Mixed Elements,' *Finite Elem. Anal. Design*, **21**, 45-74, 1995.

44. C. A. Felippa and K. C. Park, 'A direct flexibility method,' *Comp. Meth. Appl. Mech. Engrg.*, **149**, 319–337, 1997.

45. R. H. Gallagher, Private communication to K. C. Park, 1997

46. C. A. Felippa, 'Recent developments in parametrized variational principles for mechanics,' *Computational Mechanics*, **18**, 159–174, 1996.

47. Reich, G. W. and Park, K. C. (2001), "A Theory for Strain-Based Structural System Identification," in: *Journal of Applied Mechanics*, **68(4)**, 521-527.

48. K. C. Park and G. W. Reich, 'A procedure to determine accurate rotations from measured strains and displacements for system identification,' Center for Aerospace Structures, Report No. CU-CAS-98-16, University of Colorado, Boulder, CO, July 1998; *Proc. 17th International Modal Analysis Conference*, 8-11 February 1999, Kissimmee, FL.

49. K. C. Park, C. A. Felippa and R. Ohayon, 'Partitioned Formulation of Internal Fluid-Structure Interaction Problems via Localized Lagrange Multipliers,' *Computer Methods in Applied Mechanics and Engineering*, 190(24-25), 2001, 2989-3007.

50. Park K. C. and Park, Yong Hwa, "Partitioned Component Mode Synthesis via A Flexibility Approach," to appear in the June Issue of *AIAA Journal*, 2004.

51. Park, K. C., Felippa, C. A. and Ohayon, R., "Reduced-Order Partitioned Modeling of Coupled Systems: Formulation and Computational Algorithms," *Proc. NATO-ARW Workshop on Multi-physics and Multi-scale Computer Models in Non-linear Analysis and Optimal Design of Engineering Structures Under Extreme Conditions*, Bled, slovenia, June 13-17, 2004.